Chapter 2
Seismic Monitoring of Structures and New Developments

Mehmet Çelebi

Abstract Presented in this paper is an overview of the seismic monitoring issues as practiced in the past, as well as current applications and new developments to meet the needs of the engineering and user community. A number of examples exhibit the most recent applications that can be used for verification of design (including performance based design) and construction practices, real-time applications for assessing the functionality, damage condition of built environment and understanding the behavior of a particular building during strong and low-amplitude excitations. In addition and in particular, recent developments and approaches to obtain displacements and, in turn, drift ratios, in real-time or near real-time that are related to damage condition and therefore functionality of a structure are introduced. Development of wireless sensors that are now finding limited but growing applications in projects that require long-term monitoring are discussed with an example. Other special instrumentation arrays that include additional sensors to study soil-structure interaction and wave propagation are described with available recorded data.

Keywords Seismic monitoring • Structural behavior • Performance • Soil-structure interaction • Acceleration • Drift ratio • Displacement • Instrumentation

2.1 Introduction

Seismic monitoring of structural systems constitutes an integral part of the National Earthquake Hazard Reduction Program in the United States and similar hazard reduction strategies in seismically active regions of the world. In addition to the

M. Çelebi (✉)
USGS (MS977), 345 Middlefield Rd, Menlo Park, CA 94025, USA
e-mail: celebi@usgs.gov

M. Garevski (ed.), *Earthquakes and Health Monitoring of Civil Structures*,
Springer Environmental Science and Engineering, DOI 10.1007/978-94-007-5182-8_2,

United States, extensive seismic monitoring of structures programs have been established in Japan, China, Taiwan, Korea and Mexico. Other active programs exist in Italy, Turkey, Greece and Chile.

An instrumented structure should provide enough information to (a) reconstruct the response of the structure in sufficient detail to compare it with the response predicted by mathematical models and with those observed in laboratories, the goal being to improve the models, (b) make it possible to explain the reasons for any damage to the structure, and (c) to facilitate decisions to retrofit/strengthen the structural systems when warranted.

In general, and until recently, accelerometers have been used to capture the time-variant level of shaking at strategically selected orientations and locations within a structure. In addition, a structural array should include, if feasible, an associated free-field tri-axial accelerograph so that the interaction between the soil and the structure can be quantified. Recordings of acceleration responses from instrumented structures have served the scientific and engineering community well and have been useful in assessing design/analysis procedures, improving code provisions, and in correlating the system response with damage. Unfortunately, there are only a few records from damaged instrumented structures to facilitate studies of the initiation and progression of damage during strong shaking (e.g. Imperial County Services Building during the 1979 Imperial Valley earthquake, (Rojahn and Mork 1981)).

Recent trends in the development of performance-based earthquake resistant design methods, related needs of the engineering community, and advances in computation, communication and data transmission capabilities have prompted development of new goals and approaches for structural monitoring. In particular, such goals now include (a) verification of performance-based design methods and (b) needs of owners to rapidly, informedly and accurately assess the damage condition, and therefore the functionality of a building during and soon after an event. Such assessment of the damage condition or performance of a building is of paramount importance to stakeholders, which include owners, leasers, permanent and/or temporary occupants, city officials and rescue teams that are concerned with safety of those in the building, and those that may be affected in nearby buildings and infrastructures. These stakeholders will require answers to key questions such as: (a) Is there visible or hidden damage? (b) If damage occurred, what is its extent? (c) Does the damage threaten other neighboring structures? (d) Can the structure be occupied immediately without compromising life safety or is life safety questionable? As a result, property damage and economic loss due to lack of permit to enter and/or re-occupy a building may be significant. Hence, rapid and accurate assessments of the performance of a structure require measurements of displacement rather than (or in addition to) accelerations, as is more commonly done.

However, the development of new monitoring tools is being driven not only by the evolving needs of engineers but also by the advent of data acquisition systems with specific software that can record, digitize and process accelerations, integrate accelerations to obtain displacements in near real-time, and transmit both accelerations and displacements in real-time or near real-time. Such advances allow packaging structural health monitoring algorithms to meet stakeholders' needs as described above.

This paper describes the past and current status of the structural instrumentation applications for seismic monitoring and new developments. The scope of the paper also includes the following issues: (a) types of current building arrays and responses to be captured, (b) recent developments in instrument technology and implications, and (c) issues for the future. The scope does not include detailed cost considerations.

2.2 U.S. Historical Perspective and Statistics

In the United States, the California Strong Motion Instrumentation Program (CSMIP) of the California Geological Survey and the United States Geological Survey (USGS) manage the largest two structural instrumentation programs. The program operated by USGS is a nationwide cooperative effort with several states and governmental organizations (e.g. General Services Administration and Veterans Administration). Separately, some municipalities and private organizations and private enterprises have supported limited instrumentation programs aimed at their own properties and infrastructures (e.g., the Pacific Gas and Electric Company and a few financial institutions). Until recently, these programs have aimed to facilitate only response studies in order to improve our understanding of the behavior and potential for damage to structures under the dynamic loads caused by earthquakes. The principal objective of these programs has been the quantitative measurement of structural response to strong and possibly damaging ground motions for purposes of improving seismic design codes and construction practices. Detailed procedures and overall description used by the USGS structural instrumentation program are described by Çelebi (2000, 2001a). CSMIP aims to cover a wide variety of structural systems according to a predefined matrix of types of structures (Huang and Shakal 2001; Shakal et al. 2001).

CSMIP has instrumented approximately 200 buildings, 27 dams, 66 bridges and additional 42 geotechnical arrays and special structures only in California (Anthony Shakal, *pers. comm.* 2008). USGS has instrumented approximately 130 buildings and 77 dams, bridges and special structures. With the launching of the Advanced National Seismic System (ANSS 1999) authorized by U.S. Congress in 1999 (USGS 1988) and administered by USGS, as funds are appropriated, more and more structures are being instrumented throughout seismic areas of the United States. One of the criteria used by ANSS in establishing plans for the geographical distribution of instruments on structures, is population exposure to earthquake hazards (e.g., COSMOS 2001).

In general, it has not been the dominant objective of either instrumentation program to create a health monitoring environment for structures. However, recent developments in feasible sensors and recorder systems is changing the applications to include health monitoring. Data from both programs are readily available through the internet.[1]

[1] USGS data are available via www.nsmp.wr.usgs.gov and CSMIP data are available via www.consrv.ca.gov/cgs/smip. Both are accessible via www.cosmos-eq.org and www.strongmotioncenter.org

Except for a few cases that can be described as array deployments with real-time data transmittal capabilities that serve special purposes (an example of which is provided later in the paper), the overwhelming majority of the deployments follow the non-telemetered (hereinafter called "classical") method whereby the data is not transmitted in real-time.

It should be mentioned that obtaining strong-shaking data from structures requires patience and expenditures, as strong-shaking (e.g. $M > 6.0$) in even the most seismic urban environments occurs with return periods normally in decades. However, even in the absence of strong shaking, in some cases, permanent instrumentation of structures can be used to obtain low-amplitude shaking data either from small earthquakes, large earthquakes that originate at large distances to instrumented structures, ambient vibrations or forced vibrations.

2.3 General Seismic Instrumentation Issues

2.3.1 Data Utilization

Ultimately, the types and extent of instrumentation must be tailored to how the data acquired during future earthquakes will be utilized, even though there may be more than one objective for instrumentation of a structure. Table 2.1 summarizes some data utilization objectives with sample references.

2.3.2 Code Versus Extensive Instrumentation

Until 2000, the most widely used code in the United States, the Uniform Building Code (UBC-1997 and prior editions), recommended, for seismic zones 3 and 4, a minimum of three tri-axial accelerographs be placed in every building over six stories with an aggregate floor area of 60,000 sq ft or more and in every building over ten stories regardless of the floor area. The purpose of this recommendation by the UBC was to monitor rather than to analyze the complete response modes and characteristics. UBC recommended instrumentation is illustrated in Fig. 2.1a. However, this recommendation was not easily or uniformly followed. For example, following the 1971 San Fernando earthquake, in 1982, the code requirement in Los Angeles was reduced to one tri-axial accelerometer at the roof (or top floor) of a building meeting the aforementioned size requirements (Darragh et al. 1994). Later, the recommendation in City of Los Angeles was changed again similar to the original UBC recommendation but improved for taller buildings.

Beginning in 2000, International Building Code (IBC) started replacing UBC. Until recently, IBC did not have provisions for seismic instrumentation. However, the IBC 2012 will have an Appendix L that will include provisions for non-mandatory seismic instrumentation recommendation similar to that in the UBC described earlier (*personal communication*, Bachmann 2011).

Table 2.1 Sample list of data utilization objectives and sample references

Data utilization objective	Sample references and comments
Generic utilization	
Verification of mathematical models (usually routinely performed)	Boroschek et al. (1990)
Comparison of design criteria vs. actual response	Usually routinely performed
Verification of new guidelines and code provisions	Hamburger (1997)
Identification of structural characteristics (Period, damping, mode shapes)	Usually routinely performed Çelebi et al. (1993)
Verification of maximum drift ratio	Astaneh et al. (1991); Çelebi (1993)
Torsional response/accidental torsional response	Chopra and Goel (1991); De La Llera and Chopra (1995)
Identification of repair & retrofit needs & techniques	Crosby et al. 2004
Specific utilization	
Identification of damage and/or inelastic behavior	Rojahn and Mork (1981)
Soil-structure interaction including rocking and radiation damping	Çelebi (1996), (1997); Çelebi (2001a, b)
Response of unsymmetric structures to directivity of ground motions	Porter (1996)
Responses of structures with emerging technologies (base-isolation, visco-elastic dampers, and combination	Kelly et al. (1991); Kelly (1993); Çelebi (1995)
Structure specific behavior (*e.g.* diaphragm effects)	Boroschek and Mahin (1991); Çelebi (1994)
Development of new methods of instrumentation hardware (e.g. GPS, wireless)	Çelebi et al. (1997), (1999), (2001a,b); Straser (1997)
Improvement of site-specific design response spectra and attenuation curves	Boore et al. (1997); Campbell (1997); Sadigh et al. (1997); Abrahamson and Silva (1997)
Associated free-field records (if available) to assess site amplification, SSI and attenuation curves	Borcherdt (1993, 1994), (2002a, b); Crouse and McGuire (1996)
Verification of repair/retrofit methods	Crosby et al. (1994); Çelebi and Liu (1996)
Identification of site frequency from building records	Çelebi (2003)
Recent trends to advance utilization	
Studies of response of structures to long period motions	Hall et al. (1996)
Need for new techniques to acquire/disseminate data	Straser (1997); Çelebi (1998); Çelebi and Sanli (2002); Çelebi et al. (2004)
Verification of performance based design criteria	Future essential instrumentation work
Near fault factor	More free-field stations associated with structures needed
Comparison of strong vs weak response	Marshall et al. (1992); Çelebi (1998)
Functionality	Çelebi et al. (2004)
Health monitoring, damage detection, wave propagation and other special purpose verification	Heo et al. (1977); Sohn et al. (2003); Safak (1999); Çelebi et al. (2004); Jang et al. (2010); Cho et al. (2010)

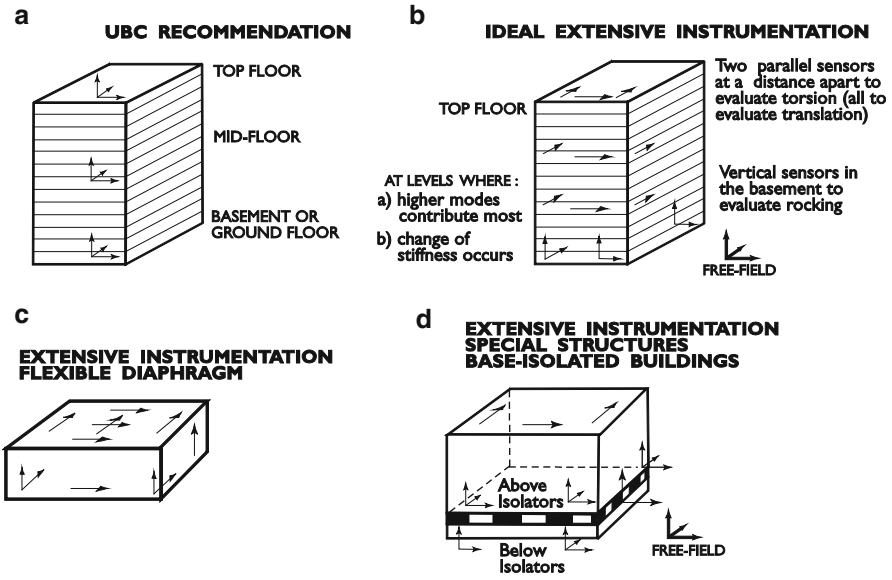

Fig. 2.1 Typical instrumentation schemes

In general, code instrumentation is naturally being de-emphasized as a result of strong desire by the structural engineering community to gather more data from instrumented structures to perform more detailed structural response studies. Experiences from past earthquakes show that the minimum guidelines established by UBC for three tri-axial accelerographs in a building are not sufficient to perform meaningful model verifications. For example, three horizontal accelerometers are required to define the (two orthogonal translational and a torsional) horizontal motions of a floor. Rojahn and Matthiesen (1977) concluded that the predominant response of a high-rise building can be described by the participation of the first four modes of each of the three sets of modes (two translations and torsion); therefore, a minimum of 12 horizontal accelerometers would be necessary to record these modes. Instrumentation needed to provide acceptable documentation of the dominant response of a structure is addressed by Hart and Rojahn (1979) and Çelebi et al. (1987). This type of instrumentation scheme is called the ideal extensive instrumentation scheme as illustrated in Fig. 2.1b.

Specially designed instrumentation arrays are needed to understand and resolve specific response problems. For example, thorough measurements of in-plane diaphragm response requires sensors in the center of the diaphragm (Fig. 2.1c) as well as at boundary locations. Performance of base-isolated systems and effectiveness of the isolators are best captured by measuring tri-axial motions above and below the isolators as well as the rest of the superstructure (Fig. 2.1d). In the case of base-isolated buildings, the main objective usually is to assess and quantify the effectiveness of the isolators. If there is no budgetary constraint, additional sensors

can be deployed between the levels above the isolator and roof to capture the behavior of intermediate floors.

Recently, during a workshop, there was consensus on "20–50 recording channels needed for detailed response definition in a building" (COSMOS 2001). With such denser deployments, reliable computations of interstory drifts (necessary for damage assessments) are possible.

2.3.3 Associated Free-Field Instrumentation

More information is required to interpret the motion of the foundation substructure relative to the ground on which it rests. This requires free-field instrumentation associated with a structure (Fig. 2.1b). However, this is not always possible in an urban environment.[2] Engineers use free-field motions as input at the foundation level, or they obtain the motion at foundation level by convolving the motion through assumed or determined layers of strata to base rock and deconvolving the motion back to foundation level. Confirmation of these processes requires downhole instrumentation near or directly beneath a structure. These downhole arrays will yield data on:

1. the characteristics of ground motion at bedrock (or acceptably stiff media) at a defined distance from a source and
2. the amplification of seismic waves in layered strata.

Downhole data from sites in the vicinity of instrumented building or other structures are especially scarce. Two new building monitoring arrays in the United States that include downhole sub-arrays are described later in the paper.

2.3.4 Record Synchronization Requirement

High-precision record synchronization must be available within a structure (and with the free-field, if applicable) if the response time histories are to be used together to reconstruct the overall behavior of the structure. Such synchronization has been achieved through extensive cabling from each individual sensor unit to the recorder. Recent technological developments enable decreasing or minimizing, and in certain cases eliminating, the use of extensive cabling. For example, global positioning system (GPS) is now widely used to synchronize building instrumentation with a separate free-field recorder; thus, eliminating cable connection between the free-field recorder and recorder within a structure. The issue here is that

[2] For example, in San Francisco, California, it is not possible to find a suitable free-field location around the Transamerica building, which is extensively instrumented.

synchronization must be an integral part of any structure monitoring scheme whether cable or wireless transmission is the means to realize it.

2.3.5 *Recording Systems, Accelerometers, Constraints and New Developments*

Before about 2005, commercially available recording systems were limited to a maximum of 12–18 channels *(e.g.* analog recorder CRA-1,[3] up to 13 channels; the digital K-2[4], 12 channels; digital Mt. Whitney[4], 18 channels). Recently, more modern versions such as Granite[4], Dolimite[4] and 130-MC[4] have been designed specifically to record and transmit via various media, including the internet, combinations of 12, 24 or 36 channels of data. Recently and in addition, PC-based data acquisition systems that utilize multiple A/D converters are developed and can accommodate several dozen channels of data. In such systems, the only constraints are the cost of the sensors and data transmission media required. One such system is described later in the chapter. Most recorders run on AC power (from mostly) one location in a building but have internal batteries to supply 12-V to the sensors via special cables that also transmit data.

Until recently, the development of and applications with wireless sensors have been very limited, mainly due to short life of batteries used as back-up power when AC power is interrupted. However, there are also new developments on this topic as reported later in the paper.

2.4 Special Arrays – Looking to the Future

2.4.1 *Special Arrays in Los Angeles, California*

Figure 2.2 shows the nine-story Millikan Library at the Caltech in Pasadena, CA and the 15-story UCLA Factor Building in Los Angeles, CA. Every floor is instrumented in these buildings with the objective of thoroughly documenting the response of a multi-story building, including the propagation of seismic waves (Safak 1999). Other special arrays have been developed for research and health monitoring applications. The special-purpose instrumentation scheme for the twin towers at Century City, in greater Los Angeles, CA is shown in Fig. 2.3. The objective of the recently-upgraded instrumentation of these two buildings is to better facilitate studies of inter-story drift, wave propagation and damage detection by recording the responses at pairs of consecutive floors.

[3] Use of commercial names or trademarks cited herein does not imply endorsement of these products by the U.S. Geological Survey.

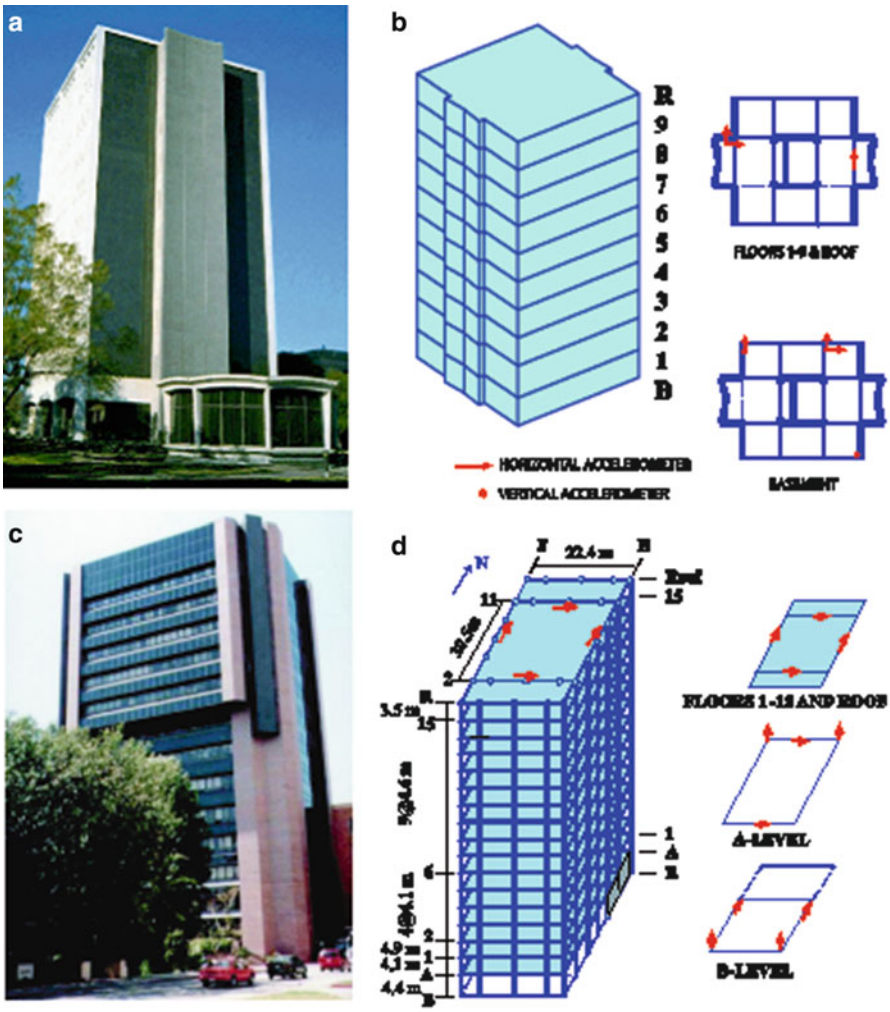

Fig. 2.2 (**a**) Millikan Library (Pasadena, CA) and (**b**) its instrumentation scheme, and (**c**) Factor Building at UCLA (Los Angeles, CA) campus and (**d**) its instrumentation scheme (Safak *pers. comm.* 2001)

2.4.2 Displacement Measurement Needs and Arrays, and Real-Time Data

Two important reasons are driving the recent push for developing technologies for measuring displacements in real-time or near real-time: (a) the evolution of performance-based design methods and procedures, which rely on displacement as the main parameter, and (b) the needs of local and state officials and prudent property owners to establish procedures for assessing the functionality of buildings and other

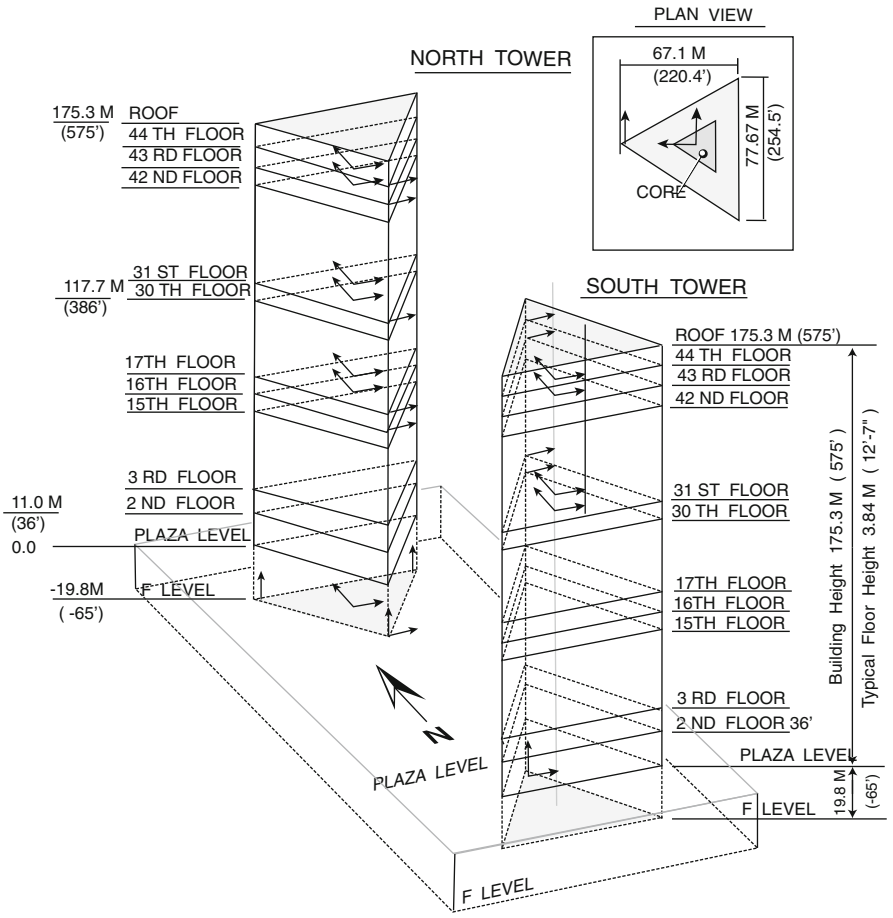

Fig. 2.3 Twin Towers of Century City (extensively instrumented for drift studies)

important structures, such as lifelines, following a significant seismic event. As a result, structural engineers increasingly want the measurement of displacements during strong shaking events in order to readily compute drift ratios that in turn are related to performance of the structure. Furthermore, such needs are driving development of ever improving monitoring methods and tools to produce data in real-time.

Until recently, assessments of damage following an earthquake were essentially carried out through inspections by city-designated engineers following procedures similar to ATC-20 tagging requirements (ATC 1989). Tagging usually involves visual inspection only, and is implemented by posting colored tags indicative of potential hazard to occupants: green indicating the building can be occupied - that is, the building does not pose a threat to life safety; yellow indicating limited occupation –that is, hazardous to life safety but not so as to prevent limited entrance to retrieve possessions; and red indicating entrance prohibited – that is, hazardous to

life. However, one of the impediments to accurately assessing the damage level of structures by visual inspection is that some serious damage may be hidden by building finishes and fireproofing. In the absence of visible damage to the building frame, most steel or reinforced concrete moment-frame buildings will be tagged based on visual indications of deformation, such as damage to partitions or glazing. Lack of certainty regarding the actual deformations may lead an inspector toward a relatively conservative tag. In such cases, expensive and time-consuming intrusive inspections may be recommended to building owners (e.g. following the $M_w = 6.7$ 1994 Northridge, CA earthquake, approximately 300 buildings ranging in height from 1 to 26 stories were subjected to costly intrusive inspection of connections ((EMA352, SAC 2000)). Thus enters the approach to real-time measurements of deformations of a structure for assessment of the structure's performance during an event. The rationale for such an approach is that, for example, a building owner and designated engineers are expected to use the response data acquired by a real-time health monitoring system to justify a reduced inspection program as compared to that which would otherwise be required by a city government for a similar non-instrumented building in the same area[4] (e.g. Program in San Francisco, CA (BORP 2001)). An example of development of such a solution and algorithm is presented later in the paper.

A challenge to meeting these objectives is the fact that dynamically measuring relative displacements between floors directly is still very difficult and, except for tests conducted in a laboratory (*e.g.*, using displacement transducers), has yet to be readily and feasibly achieved for a variety of real-life structures. However, recent technological developments have already made it possible to successfully develop and implement two approaches to dynamically measure and/or compute real-time displacements from which drift ratios or average drift ratios can be computed.

Both approaches can be used for performance evaluation of structures and can be considered as building health-monitoring applications.

The relationship between drift ratios and damage is schematically shown in Fig. 2.4. Threshold stages of damage condition as defined by drift ratios can be pre-computed using relevant structural parameters such as the type of connections and story geometry (e.g. story height). Thus, once drift ratios can be readily computed in near real-time, assessment of the damage condition of a building can be made.

2.4.3 Use of GPS for Direct Measurements of Displacements

For long-period structures such as tall buildings and long-span bridges, dynamic displacement measurements using differential Global Positioning Systems (GPS)

[4] The City of San Francisco, California, has developed a "Building Occupancy Resumption Program" (BORP 2001) whereby a pre-qualified occupancy decision-making process, as described in this paper, may be proposed to the City as a reduced inspection program and in lieu of detailed inspections by city engineers following a serious earthquake.

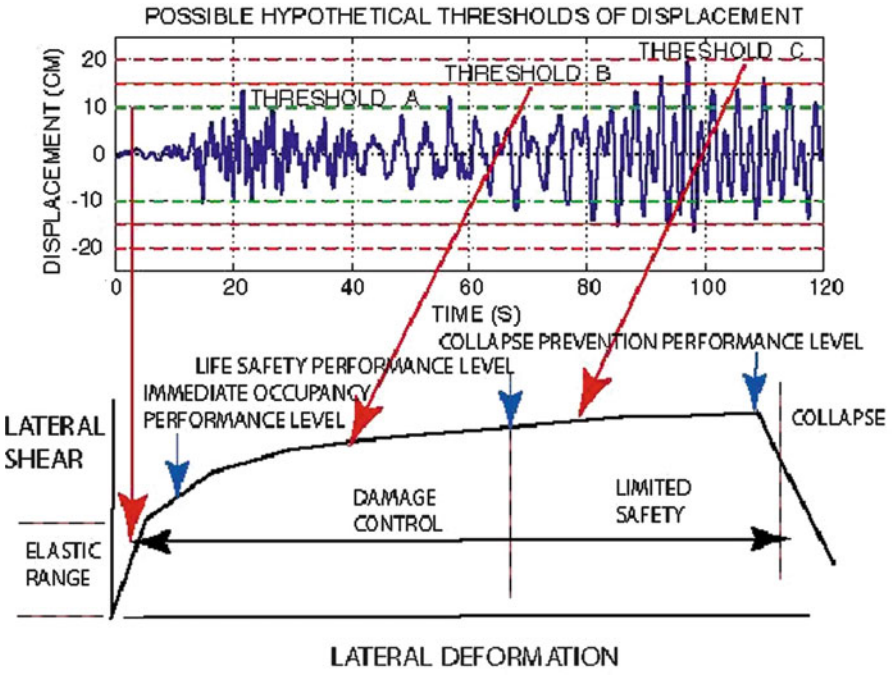

Fig. 2.4 Hypothetical displacement time-history as related to FEMA-274 (ATC 1997)

are now possible (Çelebi and Sanli 2002). However, GPS technology is limited to sampling rates of 10–20 Hz and, for buildings, these measurements are possible only at the roof.[5] A decade ago, the accuracy of measurements using the older model GPS units were ± 1 cm horizontal and ± 2 cm vertical. Current GPS units have ± 1 mm horizontal accuracy. A schematic and photos of an application in the use of GPS to directly measure displacements is shown in Fig. 2.5. In this particular case, two GPS units are used to capture both the translational and torsional response of the 34-story building in San Francisco, CA. Furthermore, at the same locations as the GPS antennas, tri-axial accelerometers are deployed to compare the displacements measured by GPS during strong-shaking events with those obtained by double-integration of the accelerometer records. Real-time acceleration and displacement data streaming in the PC-based monitoring system is also shown in Fig. 2.5.

[5] Presently up to 50 sps (samples per second) differential GPS systems with up to 50 sps are available on the market and have been successfully used to monitor drift ratios (Panagitou et al. 2006, Restrepo, personal communication, 2007) – thus enabling future usefulness of GPS to all types of structures.

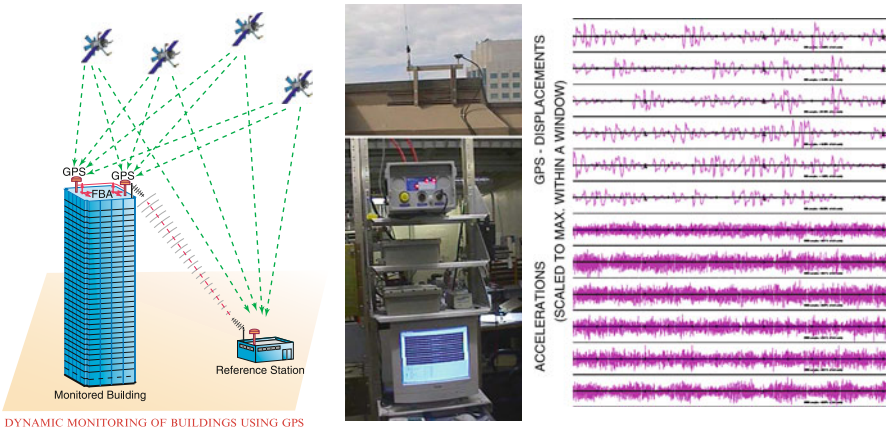

Fig. 2.5 Special instrumentation using GPS and accelerometers (San Francisco, CA.): (*Left*) Schematic of the overall system, (*Center*) GPS and radio modem antenna and the recorders connected to PC, (*Right*) streaming of acceleration and displacement data in real-time

In the absence of strong shaking data, ambient data obtained are analyzed to infer the validity of the recorded vibration signals even though the amplitudes of both the acceleration and displacement data are very small and the data is noisy (Fig. 2.6). The GPS displacement data is within the margin of error specified by the manufacturer (<1 cm. horizontal), and even then, signals are strong enough to infer structural frequencies.

In Fig. 2.7, cross-spectra (Sxy) of pairs of parallel records (north–south components of north [N_N] and south [S_N] deployments, and east–west components of north [N_E] and south [S_E] deployments) from accelerometers are calculated. The same is repeated for the differential displacement records from GPS units. The cross-spectra (Sxy) clearly indicate a dominant frequency (period) of 0.24–.25 Hz (~4 s) from both acceleration and displacement data. This frequency is within the band of expected frequency for a 34-story building. The lower amplitude peak in frequency (near ~0.1 Hz) seen in the cross-spectra of displacement records is due to noise, which is probably microseisms. It is expected that during larger amplitude motions with higher signal to noise ratios, such low frequency amplitudes due to noise will be relatively much smaller. In the acceleration data, a second frequency at 0.31 Hz is apparent. The 0.24–0.25 Hz is the fundamental translational frequency (in both directions). This is confirmed by the fact that at this frequency, the cross spectra of parallel acceleration records have a coherency of approximately unity (~1) and are in-phase (0°). On the other hand, the Sxy of parallel acceleration records at 0.31 Hz also show coherency of approximately unity but they are out of phase (180°). Therefore, this frequency corresponds to a torsional mode.

For the fundamental frequency at 0.24 Hz, the displacement data also exhibit a 0° phase angle; however, the coherencies are lower (~0.6–0.7) . The fact that the fundamental frequency (0.24 Hz) can be identified from the GPS displacement data, amplitudes of which are within the manufacturer specified error range, and that

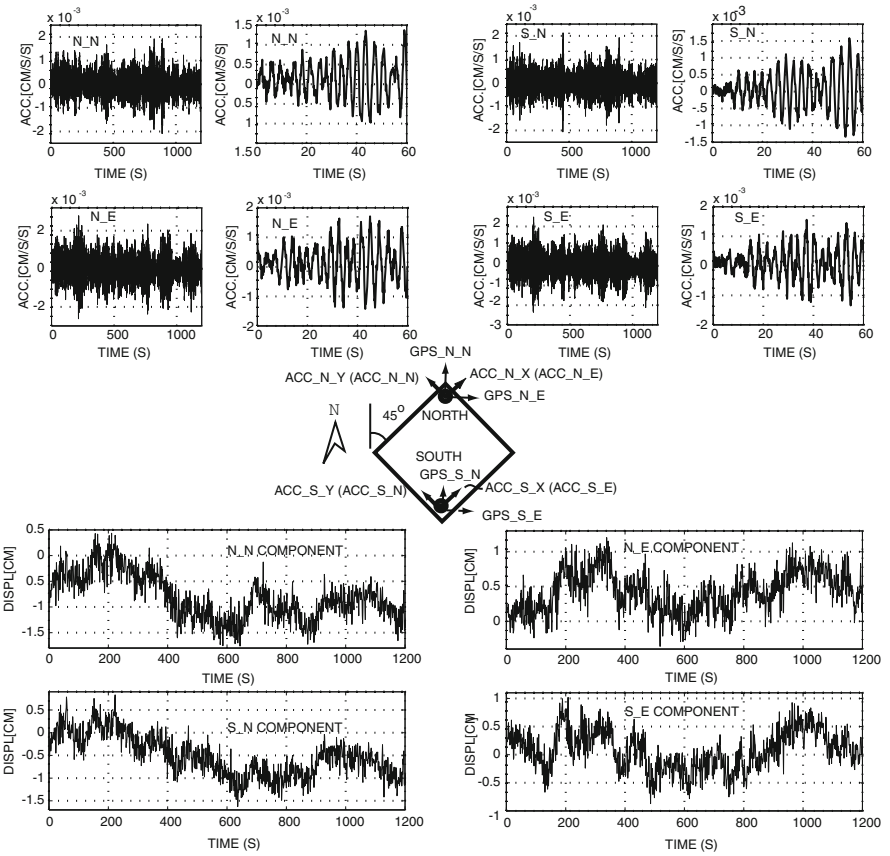

Fig. 2.6 Locations of accelerometers and GPS antennas defined in the central schematic. (*Top*) Remotely triggered and recorded ambient accelerations at N (North) and S(South) accelerometer locations. The figure shows pairs of 1,200 s long (and 60 s window from the same) record. (*Bottom*) Remotely triggered and recorded ambient displacements at N (North) and S (South) GPS Locations

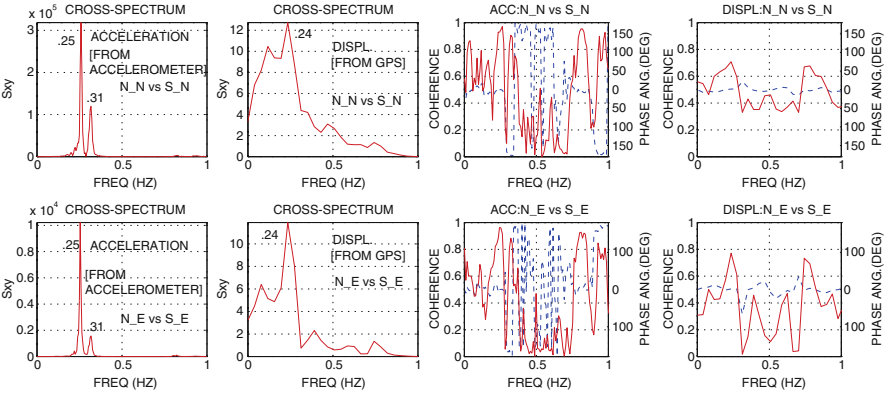

Fig. 2.7 Cross-spectra (Sxy) and associated coherency and phase angle plots of *horizontal* and *parallel* accelerations and displacements. [Note: In the coherency-phase angle plots, *solid lines* are coherency and *dashed lines* are phase-angle]

it agrees with that computed by using the acceleration data, is an indication of promise of better results when larger displacements can be recorded during strong shaking caused by earthquakes or strong winds.

Since the deployment of the pioneering GPS units in San Francisco, CA, multiple other such arrays have been developed. An important array for monitoring the wind response of five tall buildings in Chicago, IL has been developed by Kijewski-Correa and Kareem (2004).

2.4.4 Displacement via Real-Time Double Integration

As mentioned, GPS applications are currently limited to sampling at $\leq$ 20 Hz, and for building monitoring, displacement measurements (using GPS) are possible only on at the roof. This limits the application to long period structures rather than a wide variety of structural systems. Therefore, the challenge is to compute displacements from recorded acceleration responses in real-time or near real-time.

A new approach for obtaining displacements in real-time is depicted in Fig. 2.8, which also shows the distribution of 30 accelerometers in a 23-story building also in San Francisco, CA. The array is designed to provide data from several pairs of neighboring floors to facilitate drift computations. This monitoring system was primarily realized because of the needs of the building owner to utilize real-time data to meet the goals of the previously discussed BORP (2001) program in San Francisco, CA. The system has a server that (a) digitizes continuous analog acceleration data, (b) pre-processes the 1,000 sps digitized data with low-pass filters (herein called as the preliminarily filtered uncorrected data), (c) decimates the data to 200 sps and streams it locally, (d) monitors and locally records (with a pre-event memory) when prescribed triggering thresholds are exceeded, and (e) broadcasts the data continuously to remote users by high-speed internet.

The system employs software based on a general flowchart (Fig. 2.9) developed to compute displacements and drift ratios in real-time from signals of accelerometers strategically deployed throughout a building (Çelebi 2008). This approach is now implemented in several other buildings in San Francisco, CA (Çelebi 2009).

Thus, the objective of timely assessment of performance level and damage conditions of the building can be fulfilled. In addition, to facilitate studies while waiting for strong shaking events, data can also be recorded locally or remotely on demand.

The broadcast-streamed real-time acceleration data are acquired remotely using a "Client Software" configured to compute velocity, displacement and a selected number of drift ratios. Figure 2.10 shows two PC screen snapshots of the client software display configured for 12 channels of streaming acceleration or velocity or displacement or drift ratio time series. In the left frame, each paired set of acceleration response streams is displayed with a different color. In that same frame, also shown is the amplitude spectra of acceleration for one of the channels selectable by

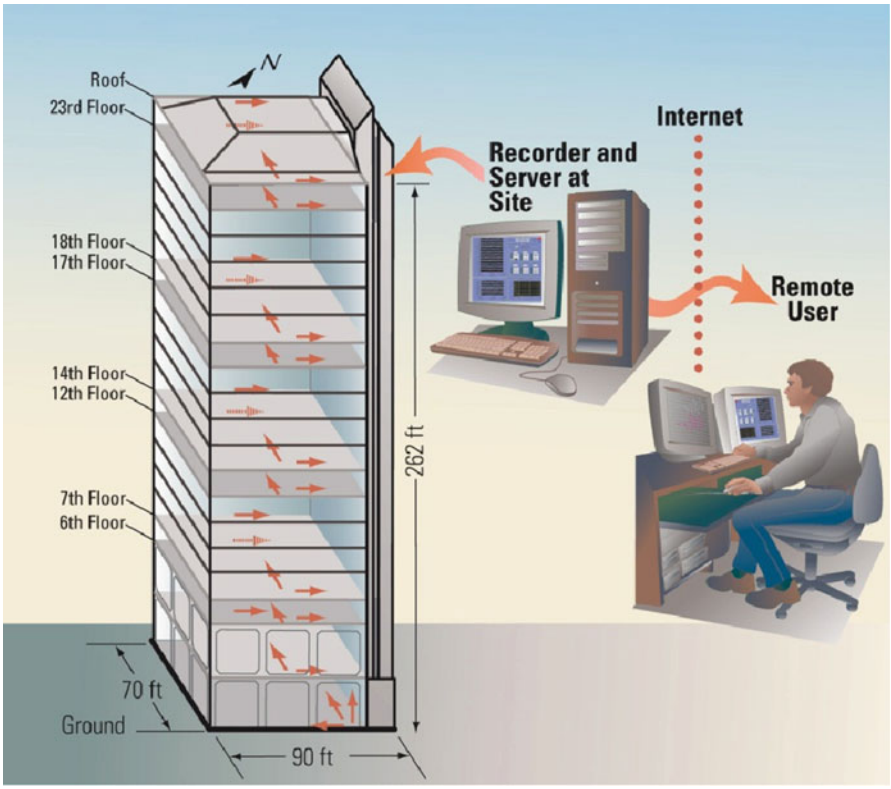

Fig. 2.8 General schematic of data acquisition and transmittal for real-time seismic monitoring of a 23-story building in San Francisco, CA

the user. It is noted that several frequency peaks are clearly identifiable (as discussed later in the chapter). In the lower left of the frame, time series of drift ratios are shown for 6 locations, each color corresponding to the same pair of data from the window above. In order to compute drift ratios, displacements are computed by real-time double integrations of filtered acceleration data. Filter options are built into the client software for processing of the acceleration data. To compute drift ratios, story heights, as shown in (the right frame of) Fig. 2.10 need to be manually entered. This figure also shows the computed pairs of displacements that are used to compute the drift ratios. Corresponding to each drift ratio, there are 4 stages of colored indicators. When only the "green" color indicator is activated, it indicates that the computed drift ratio is below the first of three specific thresholds. The thresholds of drift ratios for selected pairs of data must also be manually entered in the boxes. As drift ratios exceed the designated three thresholds, additional indicators are activated with a different color (Fig. 2.10 right). The drift ratios are calculated using data from pairs of accelerometer channels oriented in the same direction. The threshold drift ratios are computed and decided

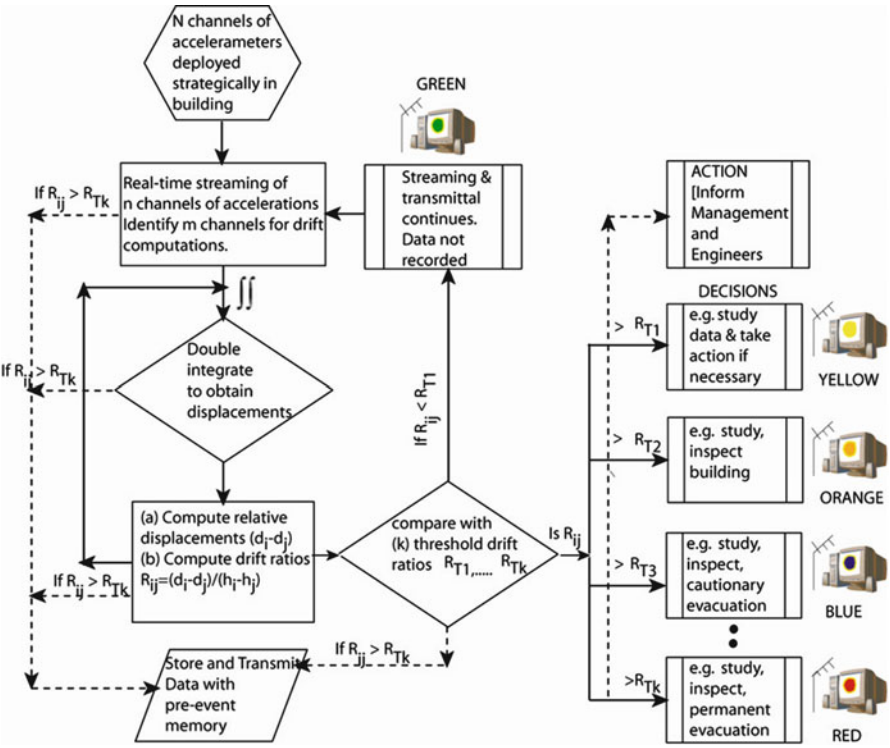

Fig. 2.9 Flow-chart for observation of damage levels based on threshold drift ratios (From Çelebi 2008)

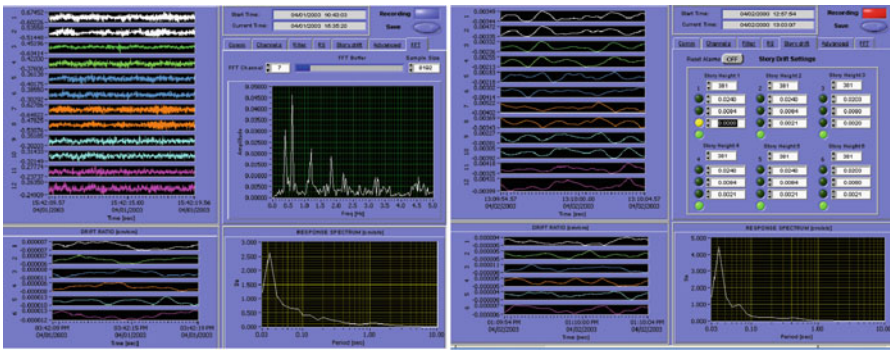

Fig. 2.10 (*Left*) Screen snapshot of client software display showing acceleration streams and computed amplitude and response spectra. (*Right*) Screen snapshot of client software display showing 12-channel (six pairs with each pair a different color) displacements and corresponding six drift ratios (each corresponding to the same color displacement) streams. Also shown to the *upper right* are alarm systems corresponding to thresholds that must be manually input. The threshold for the first drift ratio is hypothetically exceeded to indicate the starting of the recording and change in the color of the alarm from *green* to *yellow*

Table 2.2 Summary of threshold stages and corresponding drift ratios

Threshold stage	1	2	3
Adopted drift ratio	0.2%	0.8%	1.4–2.0%

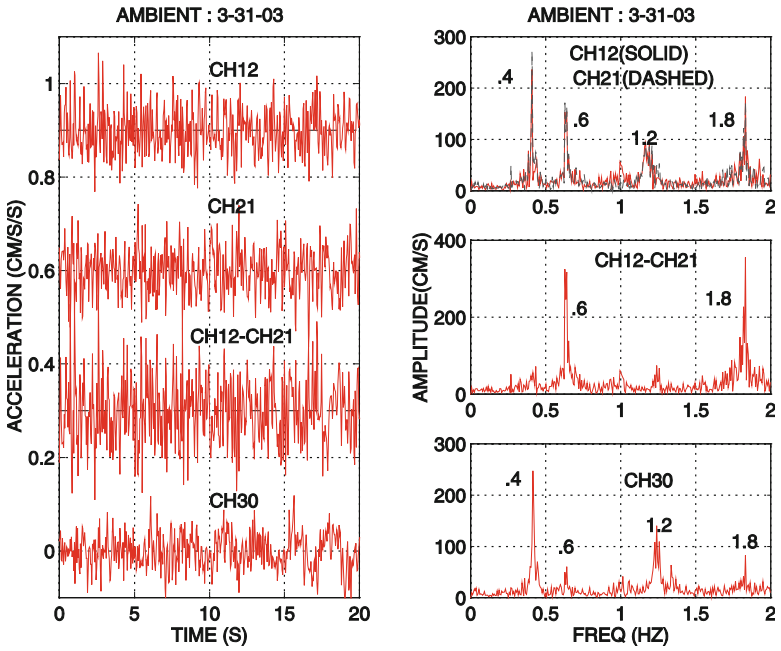

Fig. 2.11 (*Left*) Twenty seconds of ambient acceleration response data and (*Right*) corresponding amplitude spectra obtained at the roof from parallel channels (CH12 & CH21), their difference (CH12-CH21), and from CH30, orthogonal to CH12 and CH21

by structural engineers using structural information and are compatible with the performance-based theme, as illustrated in FZig. 2.4 (Figure C2-3 of *FEMA-274* (ATC 1997)) and summarized in Table 2.2 for this particular building. Figure 2.10 (right) hypothetically shows that the first level of threshold is exceeded, and the client software is recording data as indicated by the illuminated red button (in the upper right).

2.4.4.1 Sample Recorded Ambient Data and Analyses

Sample data obtained on 12 February 2003 via the client software are shown in Fig. 2.11. The data are from two parallel channels (CH12 and CH21), their difference, and an orthogonal channel (CH30) at the roof. The differential accelerations of parallel channels (CH12-CH21) identify a strong presence of torsion. The recorded peak accelerations are about 0.1–0.2 gals (~0.1–0.2 cm/s/s).

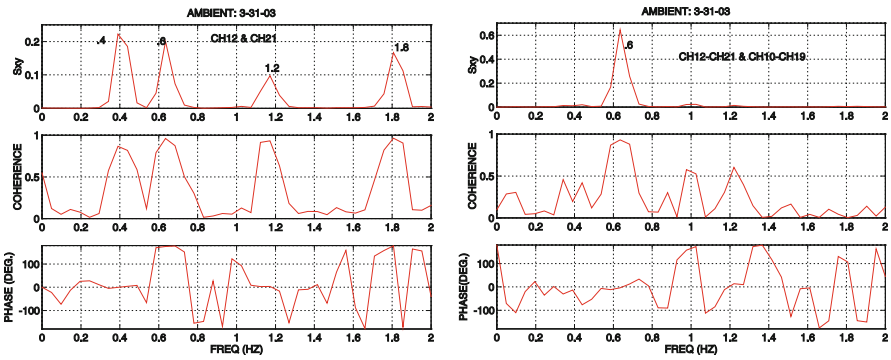

Fig. 2.12 (*Left*) Cross spectrum, coherency, and phase angle plots of ambient acceleration response data obtained from parallel channels (CH12 and CH21) at the roof. (*Right*) Cross spectrum, coherency, and phase angle plots of ambient acceleration response data obtained from differences of parallel channels, CH12-CH21 at the roof and CH10-CH19 at the 18th floor

The computed amplitude spectra clearly indicate a peak frequency for the fundamental translational mode (in both directions) at ~0.4 Hz (~2.5 s period) for all channels and at ~0.6 Hz (~1.67 s) for the torsional motion. Furthermore, the signals are good enough to identify the second translational mode at ~ 1.2 Hz (~0.83 s). Similarly, the second torsional mode is at ~ 1.8 Hz (0.56 s). The identified translational frequency is typical of a framed building that is 24 stories high. The identified modes and frequencies are further supported with the cross-spectrum, coherency, and phase angle plots in Fig. 2.12 (left). The cross spectrum, coherency, and phase angle plots of the motions recorded by CH12 and CH21 (the two parallel accelerometers at the roof level) are shown in Fig. 2.12 (left). The cross spectrum exhibits all of the significant frequencies identified in Fig. 2.11 with very high coherency (~1). At 0.4 and 1.2 Hz, the phase angles between the parallel motions are both 0°, which indicate that they are in phase and therefore belong to translational modes. At 0.6 Hz and 1.8 Hz, the phase angles are ~180° which indicate that they are out of phase and belong to torsional modes. The strong torsional response is further illustrated through Fig. 2.12 (right) which exhibits cross spectrum, coherency, and phase angle plots of the differences of motions recorded by parallel channels (CH12-CH21) at the roof and (CH10-CH19) at the 18th floor. Again, at ~ 0.6 Hz, these torsional motions exhibit significant cross-spectral amplitude with very high coherency (~1) and 0° phase angle. Therefore, 0.6 Hz belongs to the first torsional mode.

Even at the low amplitude acceleration levels exhibited in this set of sample data, the signal-to-noise ratio is satisfactory to indicate several modal frequencies. It is expected that the coherency of motions between pairs of channels will further improve when the signal-to-noise ratio is even higher during strong-shaking events. Further detailed analyses of strong shaking data will be carried out when recorded in the future.

2.4.4.2 Sample Recorded Low-Amplitude Earthquake Response Data and Analyses

During the December 22, 2003 San Simeon, CA. earthquake ($M_w = 6.4$), at an epicentral distance of 258 km., a complete set of low-amplitude earthquake response data was recorded in the building. The largest peak acceleration was approximately 1% of g. Synchronously recorded accelerations were double-integrated to obtain the displacements exhibited in Fig. 2.13 for one side of the building. Figure 2.14 further exhibits computed displacements 20–40 s into the record and reveals the propagation of waves from the ground floor to the roof. The travel time is about 0.5 s. Since the height of the building is known (80 m), the travel velocity is computed as 160 m/s. One approach for detection of possible damage to structures is by keeping track of significant changes in the travel time, since such travel of waves will be delayed if there are cracks in the structural system (Safak 1999).

As with the ambient data, in Fig. 2.15, the two parallel and orthogonal motions recorded at the roof are used to identify translational and torsional frequencies as 0.38 and 0.60 Hz respectively. Both frames in Fig. 2.16 similarly exhibit the cross-spectra (Sxy) and coherencies and phase angles at these frequencies.

Benefits of using such real-time systems for either direct measurement of displacements using GPS or real-time computation of displacements by double-integration of accelerations during very strong shaking caused by earthquakes or other extreme events are yet to be proven. However, analyses of data recorded during smaller events or low-amplitude shaking show promise.

2.5 Soil-Structure Interaction Arrays

State-of-the-art practice and analytical approaches require, when warranted, that the structure-foundation system be represented by mathematical models that include the influence of the sub-foundation media. In many cases, under a specific geotechnical environment, certain structures will respond differently than if that structure were built as a fixed-based structure on a very stiff (e.g. rock) site condition. This alteration of vibrational characteristics of structures due to soil-structure interaction (SSI) can be either beneficial or detrimental to their performance. To date, the engineering community is not clear about the pros and cons of SSI.

Adverse effects of SSI during the 1985 Michoacan (Mexico) earthquake were addressed by Tarquis and Roesset (1988), who showed that, in the lakebed zone of Mexico City, 400 km away from the epicenter, fundamental periods of mid-rise buildings (5–15 stories) lengthened due to SSI. Thus, such buildings were negatively affected due to SSI because the lengthening of their fundamental periods placed them in a resonating environment close to the approximately 2-s resonant period of the Mexico City lakebed. Conversely, under different circumstances,

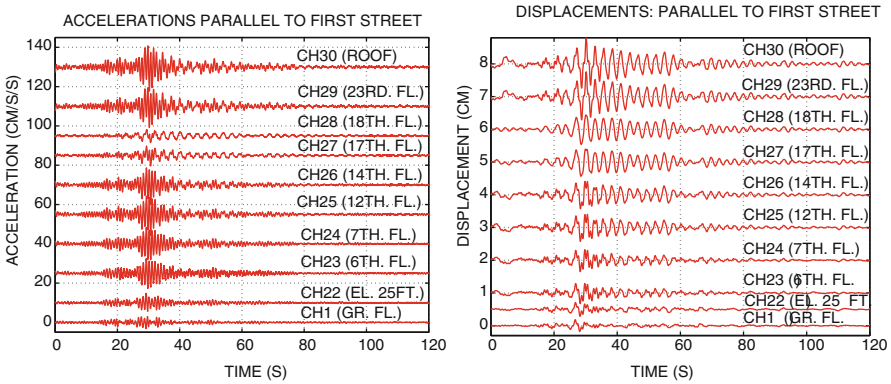

Fig. 2.13 Accelerations (*left*) and displacements derived by double-integration (*right*) at each instrumented floor (from ground floor to the roof) on one side of the building [San Simeon earthquake, December 22, 2003]

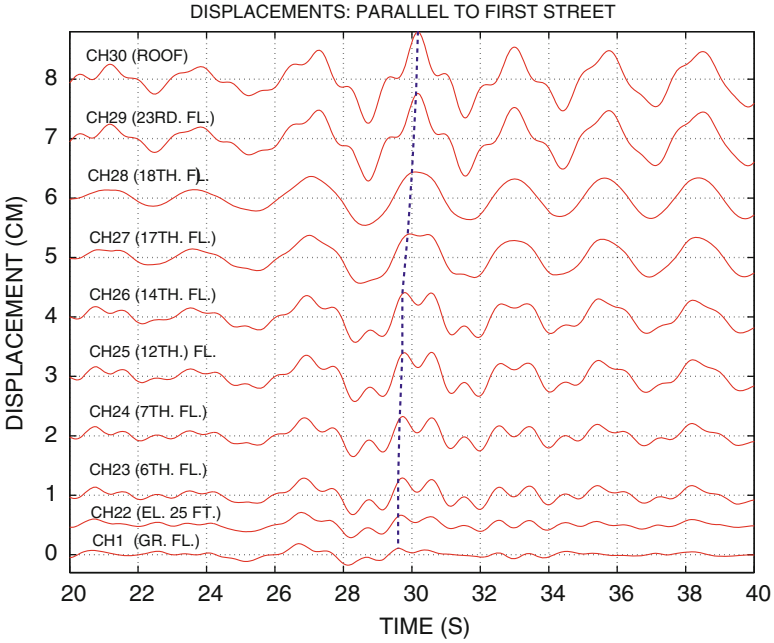

Fig. 2.14 A 22nd window plotted from 20–40 s into the record of computed displacements. Travel time of propagating vibrational waves from the ground floor to the roof of the 80 m tall building is approximately 0.5 s

SSI may be beneficial, for example, when in an appropriate geotechnical environment, a structure escapes the severity of shaking due to a shifting of its fundamental frequency.

Thus, the identification of the circumstances under which SSI is beneficial or detrimental and the relevant controlling parameters is a necessity. In-situ and

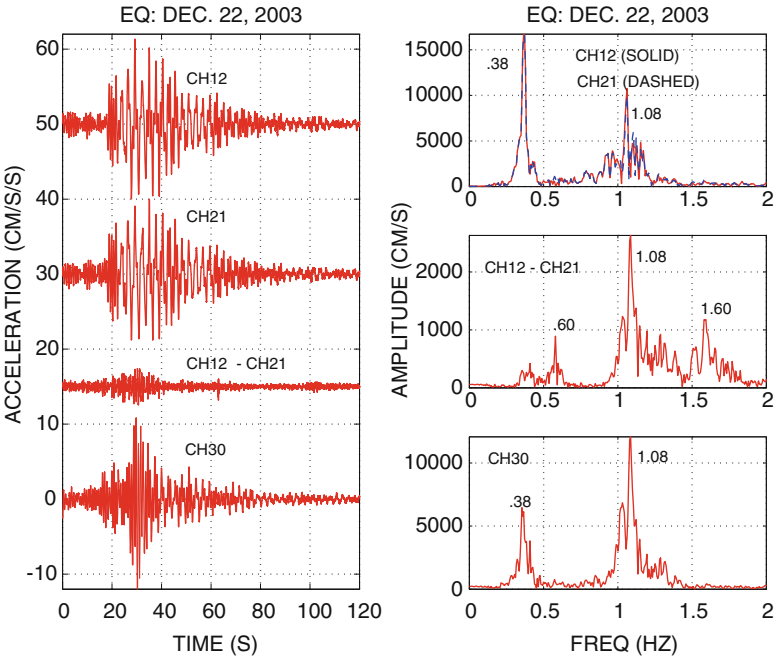

Fig. 2.15 Acceleration response data (San Simeon, CA earthquake of December 22, 2003) obtained at the roof from parallel channels (CH12 & CH21), their difference (CH12-CH21), and from CH30, orthogonal to CH12 and CH21 (*left*) and corresponding amplitude spectra (*right*)

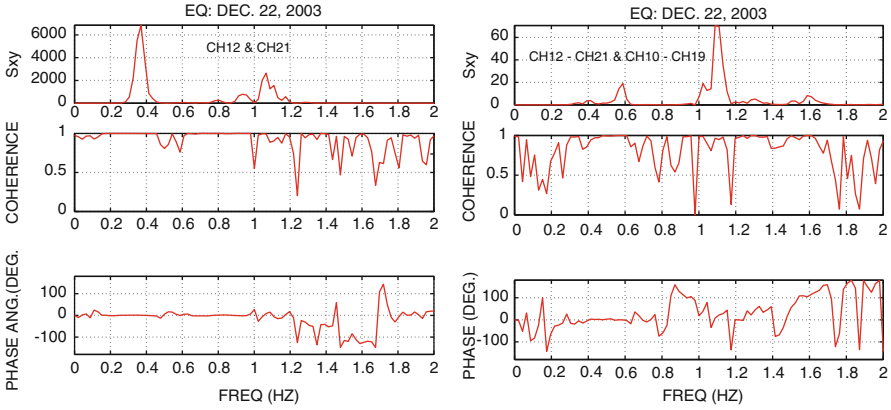

Fig. 2.16 (*Left*) Cross spectrum, coherency, and phase angle plots of ambient acceleration response data obtained from parallel channels (CH12 and CH21) at the roof. (*Right*) Cross spectrum, coherency, and phase angle plots of ambient acceleration response data obtained from differences of parallel channels, CH12-CH21 at the roof and CH10-CH19 at the 18th floor

on-scale measurements of soil-structure interaction effects are required to fully understand the response of a major structure. In turn, such measurements to capture SSI effects can be accomplished by careful planning the deployment of sensors in addition to the number of sensors deployed to capture only the response of the superstructure. Such an integrated array could include the following components:

1. the superstructure array, consisting of sensors distributed within the floors of a building to capture its translational and torsional motions,
2. the foundation array, to include sensors not only within the building and on the foundation but also beneath and on the outside sidewalls of the foundation to capture the variation of accelerations, displacements and pressures in the horizontal and vertical directions [*e.g.*, if vertical motion and rocking are expected to be significant and need to be recorded, at least three vertical accelerometers are required at the basement level (Fig. 2.1b)],
3. the spatial arrays including a vertical downhole array below or in the immediate vicinity of the structure and, a horizontal array in the immediate vicinity of the structure. Horizontal and vertical spatial downhole sensors will provide information on how the motions change while traveling through the media, and how much they are affected by the building response.

Specialized arrays that will capture SSI effects will further advance the verification of SSI effects that are currently very much limited to theoretical studies. Detailed proposals for soil-structure interaction experiments resulting from a workshop are presented in USGS OFR-92-295 (Çelebi et al. 1992). Two structural instrumentation arrays that include parts of the sub-arrays described above are now operational and promise to yield data for SSI research.

2.5.1 Transamerica Building, San Francisco, CA

One of the existing structural arrays is in the Transamerica Building, a landmark in San Francisco, CA. Fig. 2.17 shows a photo of the building.

The Transamerica Building was designed according to code requirements in force in 1972; however, design evaluation was made using a site-specific design response spectrum with seismic forces that were higher than the code requirements (Clough, R., personal communication 1990). The pyramid-shaped, steel Transamerica Building is sixty stories, 257.3 m (844 ft) high and square in plan. At the ground level, the plan dimensions are 53 × 53 m (174 × 174 ft). This plan area starts reducing at the second floor to 44 × 44 m (145 × 145 ft) at the fifth floor and then follows an exterior wall slope of 1–11 upwards. A perimeter truss system decorates and supports the building between the second and fifth floors. In addition to the exterior frame system, interior frames extend to the top of the structure with some of them ending at the 17th and 45th floors. The exterior pre-cast concrete panels are attached structurally to the exterior frames. The basement (three levels

Fig. 2.17 Photo of Transamerica Building, San Francisco, CA

below the ground level) consists of a very rigid shear wall box system. The foundation of the building consists of a 2.7 m (9 ft.) thick basemat without piles. The underlying soil media below the foundation consists, in general, of clays and dense sands. Below the ground level down to a depth of 8 m (25 ft.), there is weak and compressible sand and rubble fill and recent bay deposits of sand and clay. Below 20 m (60 ft.), the sands are partially cemented. The bedrock is between 48 and 60 m (145–185 ft.) below the present street grade.

Through an array of strong-motion instruments deployed by USGS in 1985, the response of the Transamerica Building was recorded during the October 17, 1989 Loma Prieta, CA earthquake ($M_s = 7.1$), the epicenter of which is at 97 km from building. This data set is very important as it reveals significant SSI effects associated with the earthquake response of the building. The array of instruments that recorded this effect are depicted in Fig. 2.18, which shows a three-dimensional schematic of the building, overall dimensions, the instrumentation scheme and recorded accelerations and displacements at some locations. The instrumentation scheme was designed and implemented to study the response and associated

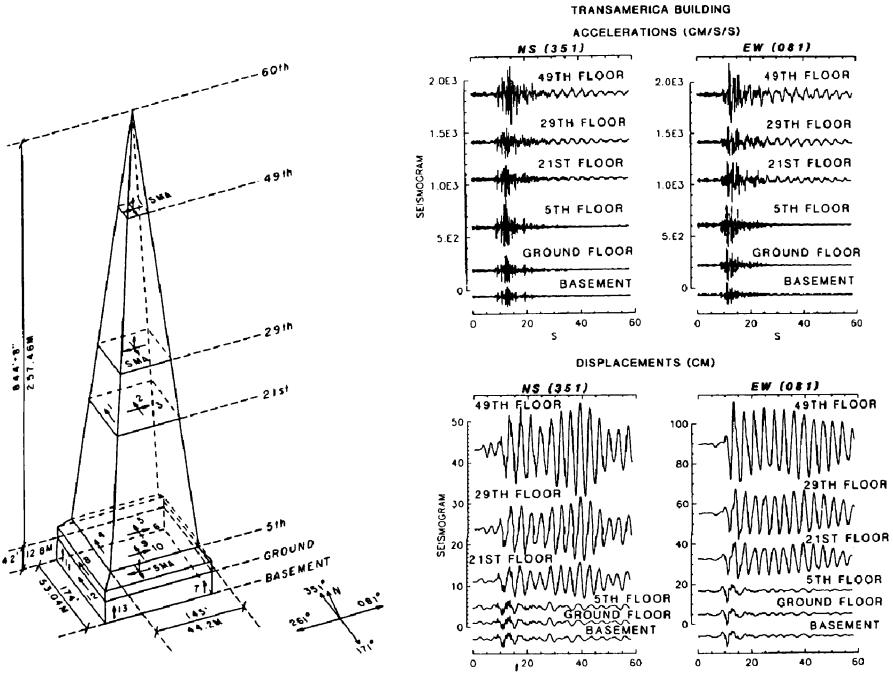

Fig. 2.18 Instrumentation schematic of Transamerica Building during the 1989 Loma Prieta (CA) earthquake and the recorded accelerations and displacements computed by double integration of accelerations. Instrumentation scheme is now upgraded

dynamic characteristics of the building, including its translational, rocking and torsional motions.[6] At the 21st, 5th and ground levels, three uniaxial accelerometers are deployed, two parallel to one another at the nominal West and East ends (nominal N-S orientation – actually 351° clockwise from true north) and the third with a nominal E-W orientation (081°clockwise from true north). These orientations are coincident with the orientations of the horizontal channels of the three SMA-1 s at the 49th, 29th and basement levels. Four uniaxial accelerometers are deployed in the basement: 3 positioned vertically at three corners of the building, and one positioned horizontally, parallel to the nominal N-S horizontal channel of the triaxial accelerograph in the basement. The orientations of the channels are also shown in Fig. 2.18. In summary, there are parallel pairs of horizontal accelerometers in each of the 21st, 5th, ground, and basement levels, and another single accelerometer deployed orthogonally to the pair in the horizontal direction at the same levels. However, because the building is in a heavily built-up area of San Francisco, there was no appropriate location for a free-field array in its immediate vicinity.

[6] The instrumentation configuration is now updated to include a modern digital recording system and uniaxial accelerometers on the 29th and 49th floors, similar to the 21st floor.

The response of the Transamerica Building during the 1989 Loma Prieta earthquake has been studied in detail (Çelebi and Safak 1991; Safak and Çelebi 1991; Çelebi 1996; 1998). The dominant frequency (or period) for the fundamental mode is 0.28 Hz (3.6 s)[7] in both the N-S and E-W directions as extracted from spectral analyses and system identification techniques. The ARX (acronym - AR for autoregressive and X for extra input) model, based on the least squares method for single input-single output, and coded in commercially available system identification software (Mathworks 1988), is used in the system identification analyses performed herein (Ljung 1987). Simply stated, the input is the basement or ground floor motion and the output is the roof level motion or motion at one of the levels where the structural response is detectable. Damping ratios are extracted with the procedures outlined by Ghanem and Shinozuka (1995) and Shinozuka and Ghanem (1995). Other modal frequencies are 0.5, 1.2, 1.5 and 1.8 Hz for the E-W direction and 1.0, 1.35, 2.0, and 2.6 Hz for N-S direction. Sample results from the application of system identification technique for the Transamerica Building records are shown in Fig. 2.19. In this application, motions at the 49th floor are used as output and those at the basemat as input (Çelebi 1996). The match between the observed and calculated response is excellent as evidenced by comparisons of the calculated and observed acceleration responses and their corresponding amplitude spectra at the 49th floor. The critical viscous damping ratios extracted from the system identification analyses corresponding to the 0.28 Hz first mode frequency are 4.9% (NS) and 2.2% (EW) (Çelebi 1996).

Analysis of the records showed that there is no significant torsional motion (Çelebi and Safak 1991).

To demonstrate the possibility of rocking, a significant contributor to SSI, horizontal motions recorded at the 21st floor and vertical motions recorded at the basemat are used. Shown in Fig. 2.20 are the coherency, phase angle and cross-spectrum for the N-S (351°) horizontal acceleration on the 21st floor and the vertical acceleration of the basemat. The rocking motion occurs at 0.5 s (or 2.0 Hz) in the N-S (351°) direction, and that at this frequency, the horizontal motion at the 21st floor and the vertical motion in the basement are coherent and in phase. This demonstrates significant and coherently identifiable rocking motion of this particular building that manifests itself in altering dynamic characteristics and response (*e.g.* lengthened period [shortened frequency] of 3.57 s [0.28 Hz] of the building as compared to those from low-amplitude tests with 2.94 s [0.34 Hz]). No SSI effects are attributable during the low-amplitude tests. Further detailed analyses of these records are provided in Çelebi (1998).

2.5.2 Atwood Building, Anchorage, Alaska

The Atwood Building is 20 stories tall and is located in downtown Anchorage, Alaska (Fig. 2.21). The building is (1) a steel moment-resisting framed structure

[7] Ambient and forced vibration tests before and ambient tests after the Loma Prieta earthquake show the fundamental period as 2.94 s (0.34 Hz) (Çelebi 1998).

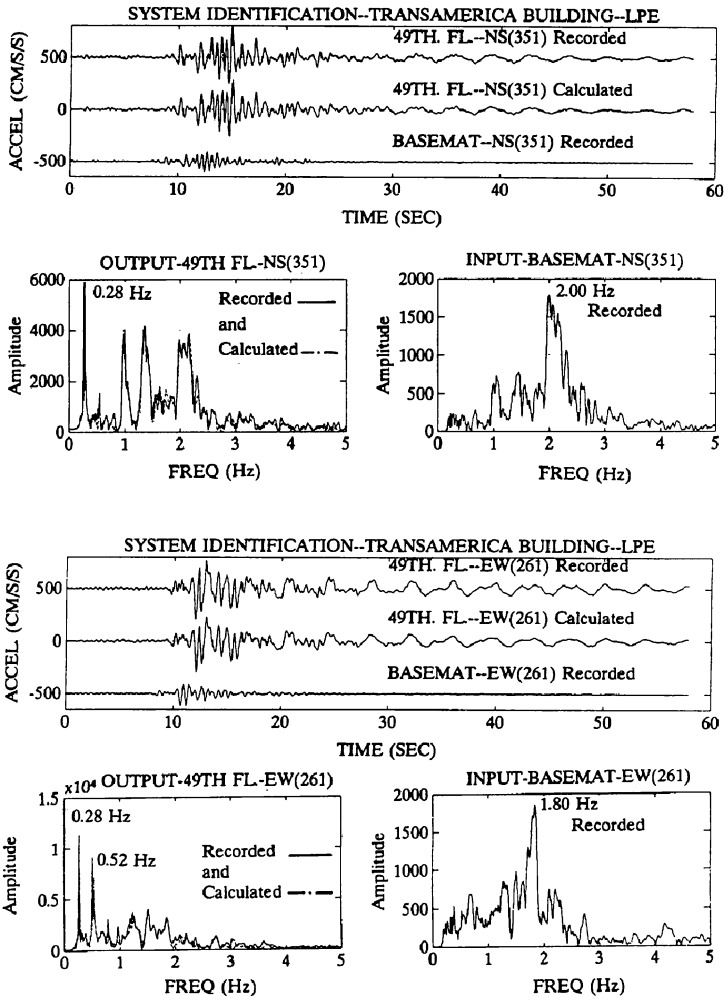

Fig. 2.19 System identification applied to motions recorded at 49th floor (*output*) and the basemat (*input*) for the Transamerica Building

with one level of basement, (2) 130 × 130′ (39.6 × 39.6 m) in plan, and (3) 264′ (80.5 m) tall. The building foundation is without any piles and consists of a 5′ (1.52 m) thick reinforced concrete mat below the core and a 4′6″ (1.37 m) thick reinforced concrete perimeter mat interconnected with grade beams.

Superstructure and foundation arrays consist of accelerometers deployed in the basement, at street level and the 2nd, 7th, 8th, 13th, 14th, 19th, (mechanical) 20th floors and roof. This configuration, depicted in Fig. 2.22, is designed to detect motion of the building in the E-W, N-S, and, (in the basement) vertical directions to capture (a) translational, (b) torsional, (c) drift ratios (displacement differences

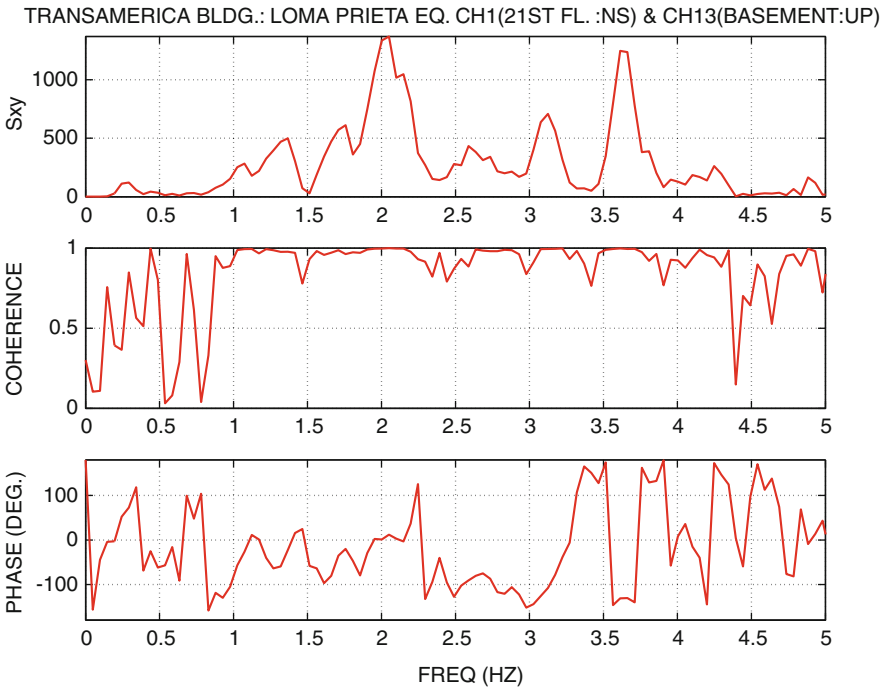

Fig. 2.20 Cross-spectrum, coherency and phase angle plots of pairs of motions (NS at 21st floor and *vertical* in the basement) indicate rocking at 2 Hz (0.5 s).

Fig. 2.21 Photo of Atwood Building, Anchorage, Alaska

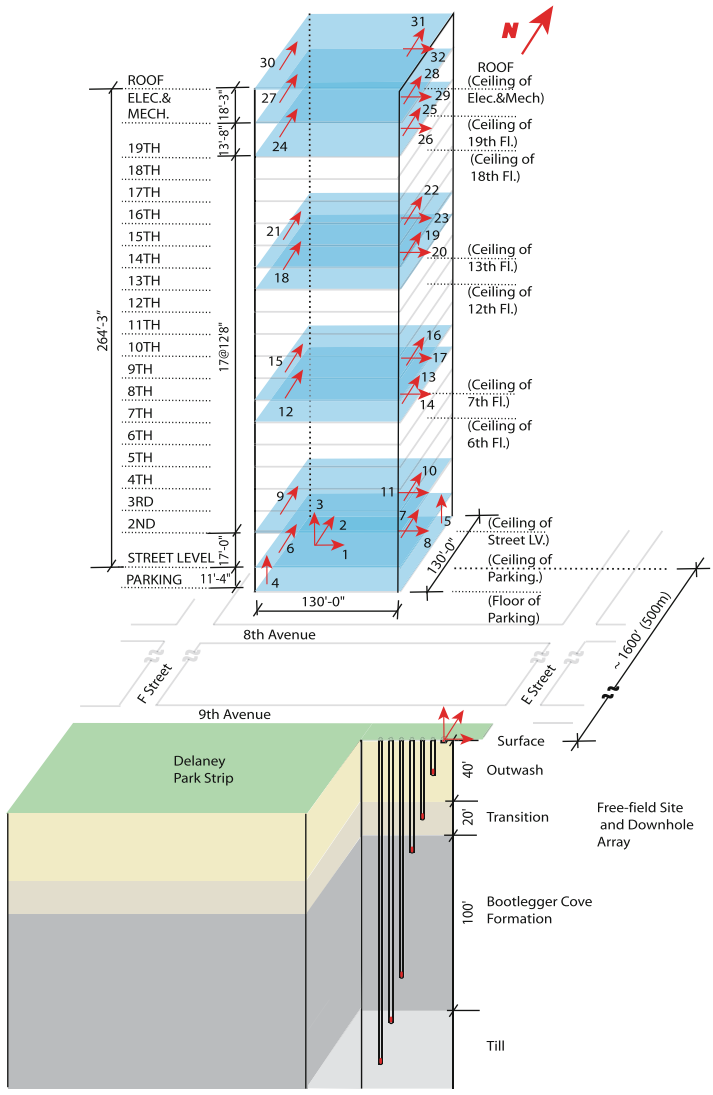

Fig. 2.22 Three-dimensional schematic of the Atwood Building (Anchorage, AK) showing the general dimensions and locations of deployed accelerometers within the structure and at free field with tri-axial downhole accelerometers. This particular building monitoring scheme is designed to capture SSI effects in addition to the traditional translational and torsional responses and has the necessary components of sub-arrays (*e.g.* superstructure, foundation, surface and downhole free-field sub-arrays)

between selected two consecutive floors) or average drift ratios (displacement differences between any two floors), and (d) rocking responses of the building.

The building array is complemented by a free-field array consisting of tri-axial surface and downhole accelerometers located approximately two city blocks from the structure – thus sufficiently removed from the vibrational effects of the building.

The associated downhole array is designed to capture the response of varying layers of soil and how such layering affects the changes in the characteristics of earthquake motions as they travel and hit the surface and affect the shaking of the structure. The downhole accelerometers of this array are deployed in six boreholes with depths ranging from 15 to 200 ft [~5–60 m] (Fig. 2.22). With the integrated downhole, surface and superstructure arrays, propagation of motions starting from the downhole to the roof of the building can be captured, allowing engineers to study the interaction between the soil and the structure.

Downtown Anchorage is underlain by an approximately 100–150-ft (30.5–45.7 m) thick soil layer known as the Bootlegger Cove Formation, where considerable ground failures occurred during the 1964 Great Alaska earthquake. For various levels of shaking, recording the response and assessing the behavior of structures at such sites and of the sites themselves is of interest to the engineering community as the next large earthquake will most likely affect the performance of structures at such sites. Detailed analyses of low-amplitude responses of the building recorded from several small amplitude earthquakes are provided in Çelebi (2006a). Only sample data recorded from the structure array is introduced below.

Accelerations and computed displacements (double-integrated accelerations) from both the site and the superstructure arrays of the Atwood Building during the April 6, 2005 Tazlina Glacier (AK) earthquake ($M_L = 4.9$, Event 18), epicenter at 183 km from the building, are shown in Figs. 2.23 and 2.24. The largest peak acceleration recorded in the building array is on the order of 0.5% g. The figures clearly show the propagation of waves from the basement to the roof of the building. The height of this building is 264 ft [~81 m] from ground floor and 275 ft [~85 m] from basement. The travel time of waves from the basement to the roof is about 0.4–0.5 s and, as expected because of the low-amplitude shaking, the propagation of the waves does not display abrupt changes (e.g. transients or spikes) to indicate damage to structural members, components and the overall structural system. Capturing the propagation characteristics and travel time is important as large and abrupt changes may indicate damage to structural members, components and system (Şafak 1999). If there are cracks in the structural system, the travel time will be longer because of the delay due to damage (Şafak 1999). In addition to displaying propagation of waves, Figs. 2.23 and 2.24 also show the beating response of the building, particularly in the NS direction displacement responses (between 80 and 100 s and also 100–120 s).

Figure 2.25 shows the roof accelerations and corresponding amplitude spectra of the two parallel NS components, their difference, and the EW component. In the spectra, significant structural frequencies [NS (0.58 and 1.83 Hz)] and EW [(.47 and 1.56 Hz)] are identified. These frequencies, and in particular predominant torsional frequencies computed from differential accelerations of parallel sensors at roof level (CH30-CH31) are better displayed in Fig. 2.26 showing spectral ratios of amplitude spectra of (a) NS and (b) EW accelerations (at the roof [CH30 and CH32] and 8th floor [CH15 and CH17] with respect to basement [CH2 and CH1] respectively) and (c) torsional accelerations at the roof [Ch30-Ch31] and 8th floor [CH15-CH16] with respect to those at the ground floor [CH5-CH7]. The torsional

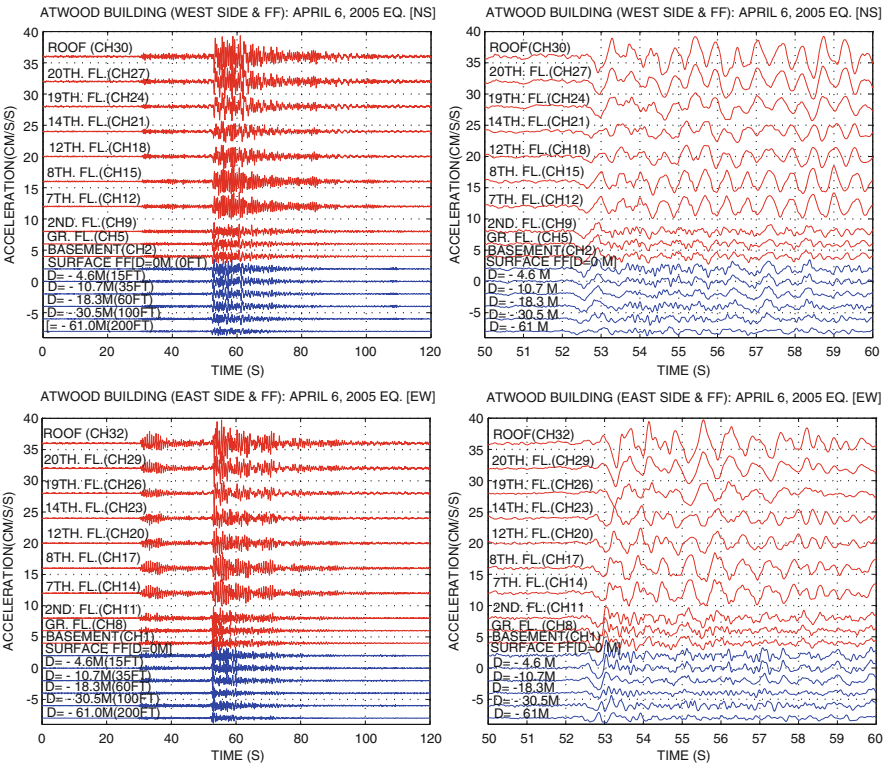

Fig. 2.23 NS (*upper panels*) and EW (*lower panels*) accelerations from both the structure and site arrays. The 10-s records on the *right* are expanded views between 50 and 60 s of the longer records on the *left*, and show in detail the propagation of S-wave from the deepest downhole to the roof of the building. (Note: vertical axes are not in scale with the vertical elevations)

frequencies [0.47–0.58 and 1.5–1.9 Hz] computed from differential accelerations (Figs. 2.25 and 2.26) are similar to the predominant frequencies computed from NS and EW roof accelerations, indicating possible coupling and also possibly causing the beating effect visually most prominent in the displacement time-history plots (Fig. 2.24). Furthermore, the narrow band of the structural frequencies in the amplitude spectra or the spectral ratios reflect the low damping ratios that is also a cause of beating effect.

Figure 2.27 presents cross-spectrum, coherence and phase angle plots of pairs of NS ([a] CH30 and CH15), EW ([b] CH32 and CH 17) and torsional (differential of NS) accelerations [c] (CH30-CH31 and CH15-CH17) at the roof and 8th floor. The pairs of accelerations in each case are perfectly coherent for the modal frequencies indicated, and are 0° in phase for the lowest frequencies (indication of first mode) and 180° out of phase for the second and third lowest frequencies (indicating second and higher modes). It is noted again that the frequencies for the torsional responses are similar to the translational frequencies.

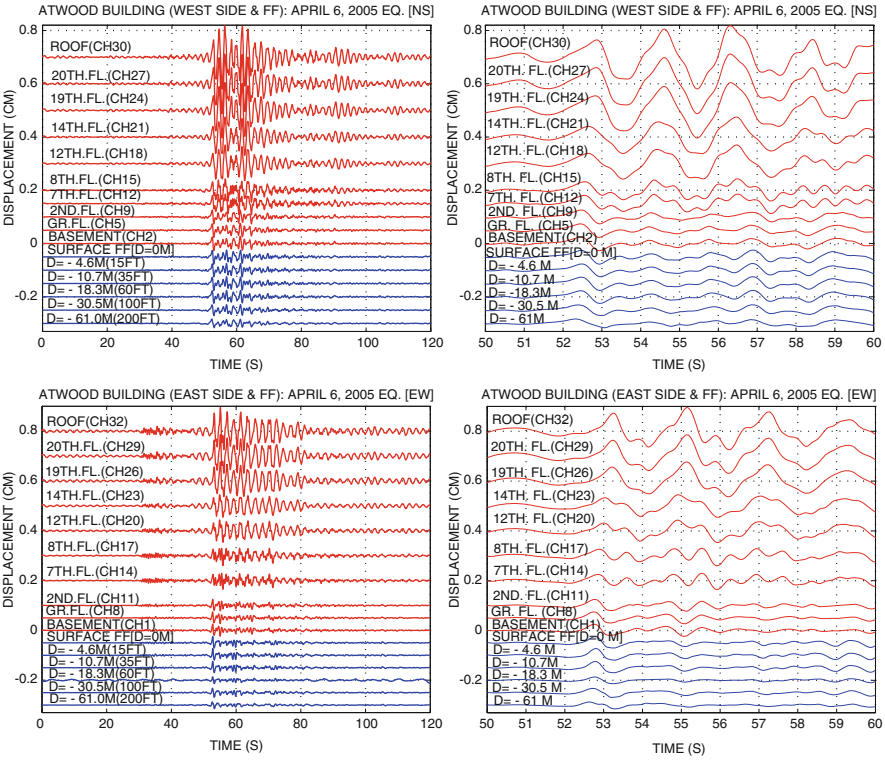

Fig. 2.24 NS and EW displacements corresponding to Fig. 2.23. (Note: vertical axes are not in scale with the vertical elevations)

No evidence of soil-structure interaction (SSI) effects was found for the low-amplitude shaking caused by this distant small earthquake. Even though the vertical motions at the basement are not identical for the three locations, no phase differences were observed. As a result, no rocking effects have been identified. Stronger shaking at the site and building from future earthquake may reveal such effects. However, the fundamental frequency of the site (1.3–1.7 Hz) is very close to the second modal frequencies of the building (1.83 Hz for NS and ~1.5 Hz for EW direction), thus inferring that resonance of the building at this mode might occur.

2.5.3 New Array in Boston, Massachusetts

In late 2010, a cast-in-place reinforced concrete building at Massachusetts Institute of Technology (MIT) Campus in Cambridge, MA was instrumented with state-of-the-art seismic monitoring system. The building, constructed in the early 1960s and opened to service in 1964, has 20 stories (87.3 m [286.5′] overall height) plus a one-story basement below ground level. The shape is rectangular in plan (14.6 m [48′] × 34 m [116.5′]) with solid shear walls extending from the

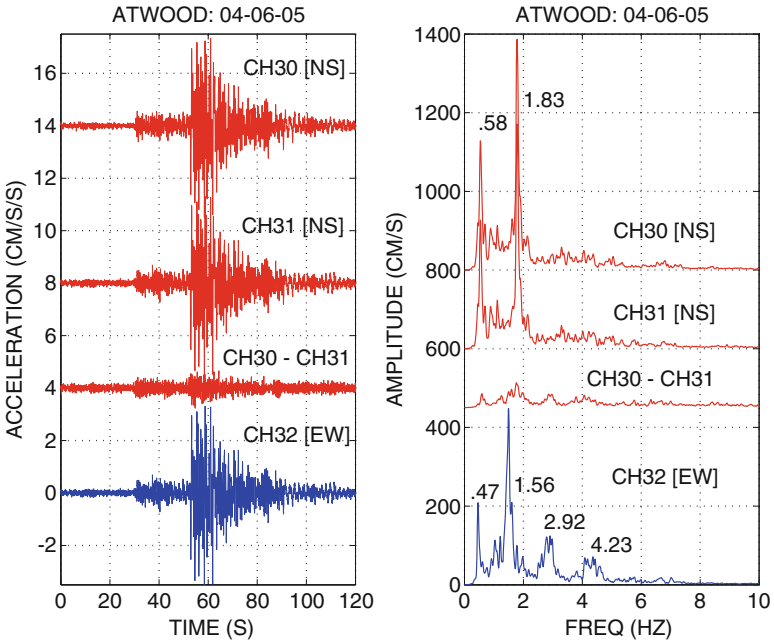

Fig. 2.25 Roof acceleration time-histories and corresponding amplitude spectra

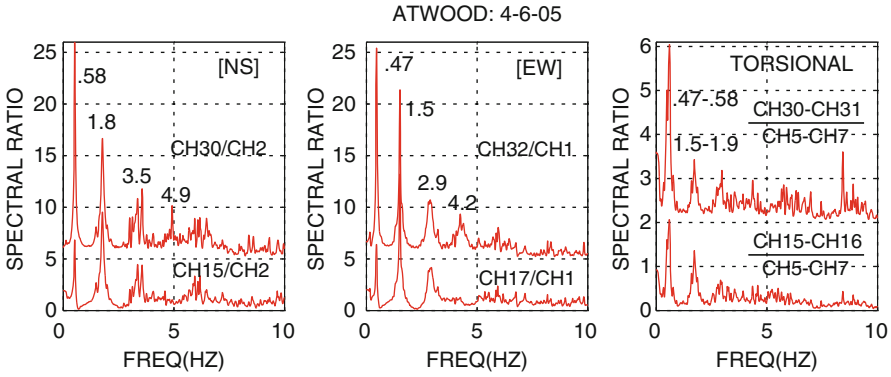

Fig. 2.26 Spectral ratios computed from amplitude spectra of NS and EW accelerations at the roof (CH30 and CH32, respectively) and 8th floor (CH15 and 17) with respect to those at basement, and torsional accelerations at the roof and 8th floor with respect to those at ground floor (CH5 and 7)

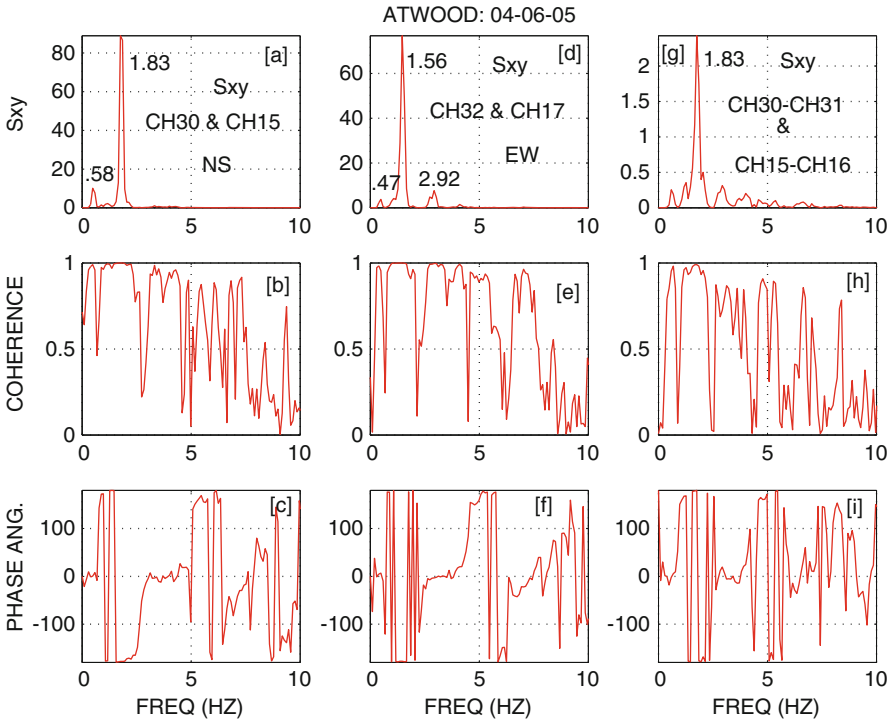

Fig. 2.27 Cross-spectrum, coherence and phase angle plots of pairs of NS (CH30 and 15), EW (CH32 and CH 17) and differential of NS accelerations (CH30-CH31 and CH15-CH17) at roof and 8th floor identifies significant frequencies and associated modes

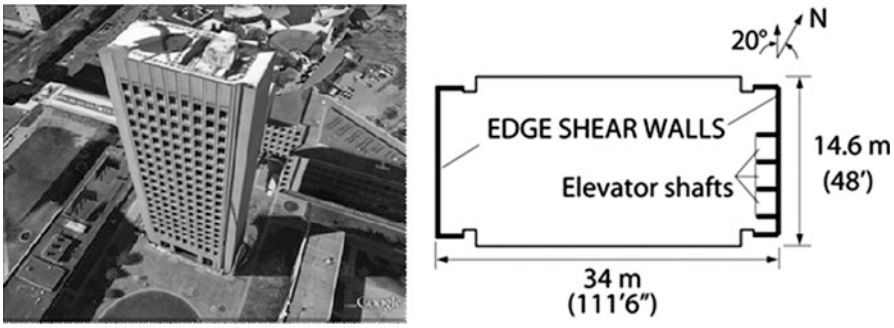

Fig. 2.28 (*Left*) Image of Building 54 at MIT Campus (captured using Google Earth©). (*Right*) Typical plan-view of the building depicting the distribution of shear walls at the western and eastern ends of the building

basement-foundation level to the roof level at the two narrow ends. The foundation system comprises individual and spread footings supported by 14-in. [36 cm] diameter piles with caps partially or totally monolithic with basement slab. A picture of the building and its typical in-plan view are presented in Fig. 2.28.

Significant features expected to influence the shaking response of the building include the monolithic shear walls at its two narrow ends, large openings in its narrow direction at ground floor level, and large and heavy equipment anchored asymmetrically at its roof. Furthermore, there are vertical discontinuities immediately above the ground level and the level above it. The top two floors (19th and 20th levels) are mechanical floors. Heavy equipment is installed asymmetrically on the roof. The narrow ends of the building are aligned at 20° ccw from true North, but, in this paper, the direction of the narrow and wider edges of the building will be referred to as the structural NS and EW directions, respectively.

Geotechnical aspects of the building site and its vicinity are well characterized. The ground surface is approximately ~6.1 m (20 ft) above sea level, and depth to bedrock is approximately 30.5–34.0 m (100–110 ft) below sea level. Available borehole logs in the vicinity of the building allowed computation of the fundamental site frequency as ~1.5 Hz (Çelebi et al. 2011). This value will be useful in assessing any site-related resonance of the building that might occur during the shaking from an earthquake or other significant excitation.

Figure 2.29 shows a schematic of the building depicting important dimensions as well as locations and orientations of the 36 (4-g) accelerometers deployed throughout the building. Each accelerometer channel is connected via cable to a 36-channel central recording system. Accurate (<1 μs) timing for data sampled at 200 Hz is synchronized to UTC by connecting to a GPS antenna deployed at the roof . The array is designed for recording (a) translational, (b) torsional and (c) rocking motions of the building, as well as for computing (d) drift ratios between adjacent floors or average drift ratios between non-adjacent floors. The capabilities of the state-of-the-art recording system include: (1) local and remotely accessible real-time data streaming, (2) adding data from pre-event memory of desired duration of an event recorded according to desired thresholds, (3) local and remote access to any data in the buffer (4) easy transmittal or retrieval event data, (5) system health monitoring and (6) on demand ambient data recording on site or remotely.

Since this array is relatively new, strong-shaking data is not available. In absence of strong shaking data, several sets of ambient data with durations of about 120–300 s were recoded. A quick check of these data indicated that the dynamic characteristics of the building appear to be repeatable at the low-amplitude motions recorded. Therefore, analyses of data from only one set that was recorded on October 28, 2010 is presented.

Figure 2.30 shows a sample time-history plot of ambient data (in relative accelerations) from the roof. As will be shown, torsion is significant in this building because the building is torsionally unbalanced, most likely due to the asymmetric shear walls around the elevator shafts on the east end of the building (Fig. 2.28). Asymmetrically installed heavy equipment at the roof and elsewhere in the building surely contributed to its significant torsional behavior.

Figure 2.31 shows relative amplitude spectra computed for the ambient acceleration data presented in Fig. 2.30. Because the ambient data has a high signal-to-noise ratio, the distinction between the lowest (fundamental) frequencies (periods) is clear [NS translation 0.75 Hz (1.33 s), EW translation 0.68 Hz (1.47 s) and torsion

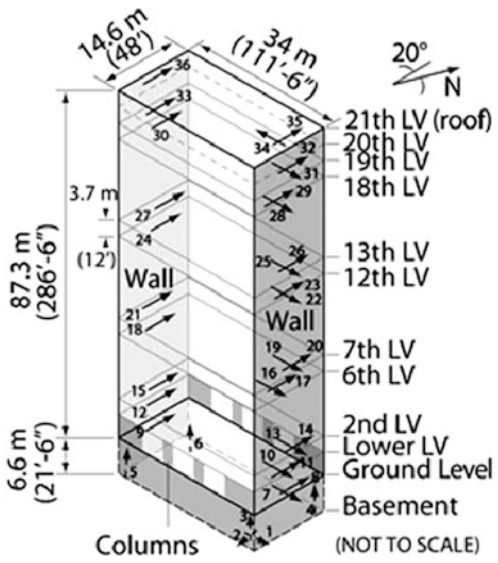

Fig. 2.29 Schematic showing accelerometers deployed throughout the various floor levels of the building. The arrows indicate the orientation of positive acceleration for each sensor. Accelerometers are located as close as possible to the east and west shear walls. Vertical accelerometers are deployed at the four corners of the basement. Level 20 (shown in *dashed lines*) is not instrumented

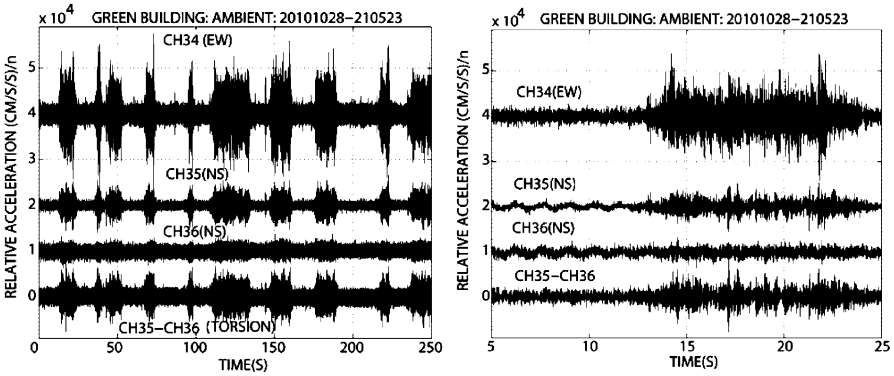

Fig. 2.30 (*Left*) Relative ambient acceleration data of 250 s duration remotely recorded on demand from the roof of the building. Relative torsional motions (at *bottom* of each frame) are indicated by the difference of two parallel channels at the roof. (*Right*) 20-s window of the same data

1.42 Hz (0.70 s)]. It is noted that torsion calculated by taking the difference of the two parallel accelerations recorded by channels (denoted CH) 35 and 36 (last curve in the upper panel of Fig. 2.31) does not show any peaks in common with the fundamental translational frequencies, thus indicating that the fundamental translational and torsional modes are not coupled. The second modes in the NS direction at ~2.6 Hz (0.39 s) and in the EW direction at ~ 2.45 Hz (0.41 s) are also visible in the spectra. The two additional plots in Fig. 2.32 further verify the identified frequencies and associated modes as explained later in this section.

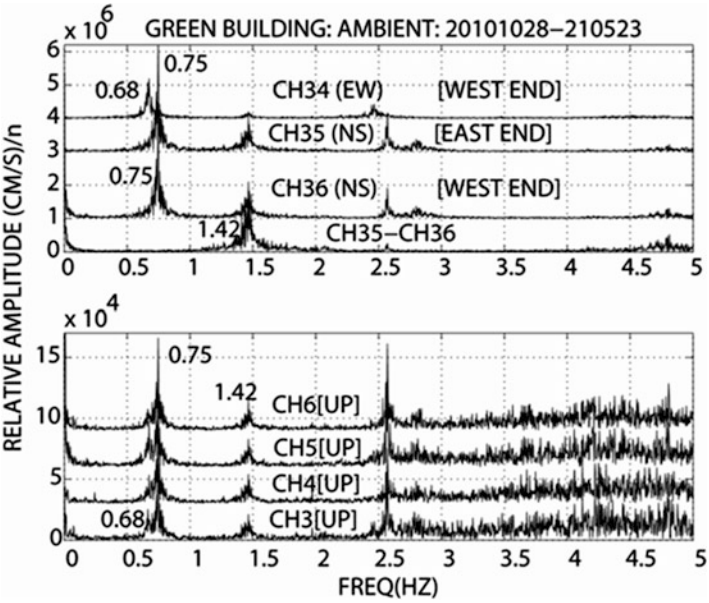

Fig. 2.31 Relative amplitude spectra of (*top frame*) horizontal motions and of torsion (*curve at bottom*) at the roof, and (*bottom frame*) vertical motions in the four corners of the basement

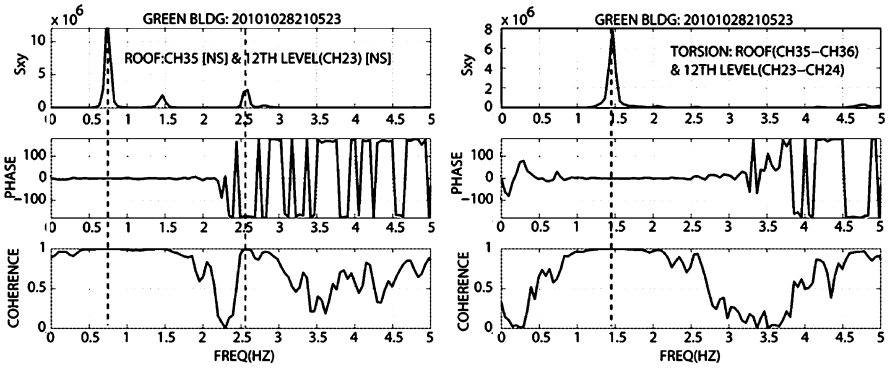

Fig. 2.32 Cross spectra, coherency and phase angles for selected components of motion. (*Left*) The fundamental and second mode frequencies at 0.75 Hz and 2.60 Hz in the NS direction are clearly illustrated using CH35 at the roof and CH23 at the 12th Level, which are highly coherent and have phase angles of 0 and 180°, respectively. The peak at ~1.4 Hz with 0° phase angle belongs to the fundamental torsional mode. (*Right*) Torsional motions at the roof (CH35-CH 36) and at 12th level (CH23-CH24). A small peak at ~4.7 Hz with 180° phase angle corresponds to the second torsional mode

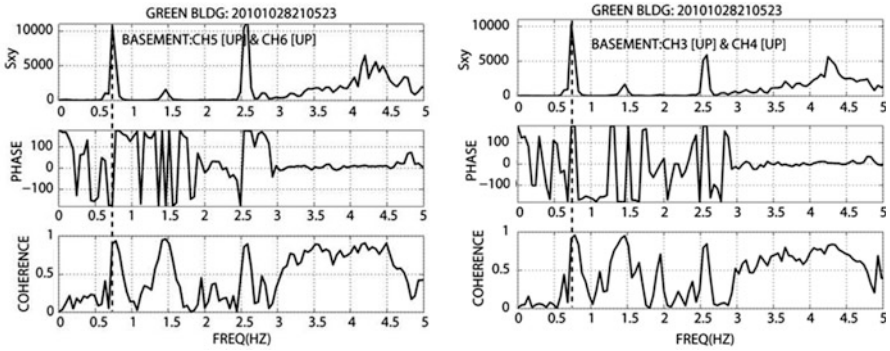

Fig. 2.33 Cross-spectra (Sxy), phase angle, and coherence for pairs (W end on the *left*, E end on the *right*) of vertical sensors in the basement. Rocking around the EW axis (NS direction) is identified on the basis of unity coherency and 180° phase angle at ~0.75 Hz and ~2.5 Hz in both plots

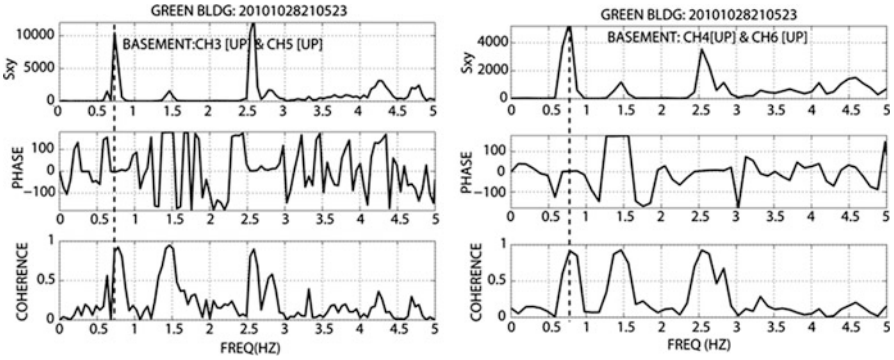

Fig. 2.34 Cross-spectra (Sxy), phase angle, and coherence for pairs (S side on the *left*, N side on the *right*) of vertical sensors in the basement. Zero phase angles and near unity coherency at ~0.75 and ~2.5 Hz (for two pairs of vertical motions around NS axis from the basement) indicate that there is no rocking in the EW direction

In the lower frame of Fig. 2.31, spectra for all four vertical components of acceleration in the basement are very similar, and exhibit frequency peaks in common with those of the horizontal translational and torsional modes (note the minor peak at 2.4 Hz that corresponds to the second mode in EW translation). This clearly indicates that the basement vertical motions are most likely influenced by the horizontal translational and torsional modes by means of rocking – a form of structure-foundation-soil interaction. This is significant in that this interaction takes place even during low-amplitude ambient shaking. (Further evidence of this interaction is shown later in the plots of cross-spectra, coherency and phase angles of Figs. 2.33 and 2.34.)

The left frame in Fig. 2.32 shows the cross-spectrum, coherency and phase angles for CH35 at the roof and CH23 at the 12th level and depicts with high

Table 2.3 Summary table of frequencies (f), periods (T) and damping percentages (ξ) determined by system identification

	Translational								
	NS			EW			Torsion		
	f	T	ξ	f	T	ξ	f	T	ξ
Mode	(Hz)	(s)	[%]	(Hz)	(s)	[%]	(Hz)	(s)	[%]
1	0.75	1.33	0.03	0.67	1.47	0.04	1.49	0.33	0.19
2	2.63	0.38	0.06	2.49	0.40	0.01	–	–	–

coherency the fundamental and second mode frequencies in the NS direction: 0.75 and 2.60 Hz with and 0 and 180° phases respectively. The peak at ~1.4 Hz belongs to the fundamental torsional motions (with 0° phase angle). This is also more clearly depicted in the right frame of Fig. 2.32 that shows cross-spectrum, coherency and phase angles for torsional motions CH35-CH36 at roof and CH23-CH24 at 12th level. A small peak at ~4.7 Hz indicates second torsional mode with 180° phase angle.

That rocking occurs in the building is demonstrated by cross-spectrum, phase angle and coherency functions between pairs of vertical motions in the basement. Figure 2.33 shows plots for two pairs of vertical motions around the EW axis (that is, rocking in the NS direction). Clearly, the peaks at ~0.75 Hz and ~2.5 Hz in the cross-spectra, which have coherency nearly equal to unity and are out of phase by 180°, indicate rocking in the NS direction. In contrast, Fig. 2.34 shows two pairs of vertical motions around NS axis, where, at the same frequencies, the motions have near-unity coherence but are in phase (0°), thus indicating no rocking around the NS axis (EW direction).

System identification analysis was performed using the ambient data to identify and/or validate key frequencies and compare them with those determined by spectral analyses. A model is estimated using appropriate pairs of recorded acceleration responses as single-input, single-output. The auto-regressive extra input (ARX) model based on least squares method is used in this analysis. The reader is referred to Ljung (1987) and Matlab User's Guide (1988 and newer versions) for detailed formulations of the ARX and other system identification models. Some of the key frequencies for four of the important modes were identified along with the corresponding modal damping ratios. These results are summarized in Table 2.3.

Thus, it is shown that, in absence of strong shaking, low-amplitude ambient vibration can be used to infer the behavior of the building and its dynamic characteristics. The data reveal distinct translational frequencies for the two major orthogonal axes (0.75 Hz NS, 0.67 Hz EW), a torsional frequency of ~1.49 Hz, and a rocking frequency around EW axis of 0.75 Hz which is same as the NS translational frequency. The fact that the two frequencies (NS translation and rocking around EW axis) are same clearly implies that motions in the NS

direction are dominated by rocking motions with little or no bending contribution. Very stiff shear walls at the east and west ends of the building and weak geotechnical layers underlying its foundation provide the best combination for soil-structure interaction in the form of rocking behavior around the east–west axis of the building. Clear evidence of such rocking behavior is rarely observed from low-amplitude data. In addition, a site frequency of ~1.5 Hz is determined from a shear wave velocity versus depth profile obtained from a borehole in the vicinity of the building. While the translational frequencies of the building are not close to the site frequency, the torsional frequency is almost identical and may have contributed to resonant behavior during which the torsional frequency of the building is injected into the horizontal and vertical motions in the basement because of the rocking. In addition, the observation that the fundamental structural frequency in the NS direction (0.75 Hz) also appears in the vertical motions of the basement suggests that these spectral peaks reflect rocking motions of the building at this frequency.

It has been observed and documented that dynamic characteristics of structures can vary considerably during strong shaking as compared to low-amplitude shaking (Çelebi 2007). Therefore, while it is likely that for this building also, the dynamic characteristics identified from the ambient motions may differ considerably during stronger motions that may be generated from nearby earthquakes or site-amplified motions from earthquakes at large distances, the study results serve as baseline to behavior and response characteristics of the building at stronger shaking.

2.6 Cape Girardeau (Bill Emerson) Bridge, MO

Figure 2.35 exhibits the cable-stayed Bill Emerson Memorial Bridge (also known as Cape Girardeau Bridge) in Cape Girardeau (Missouri, USA) which is instrumented with a monitoring system capable of streaming real-time acceleration response data that can be configured to establish performance indicators using the sensor data at the deck center or tops of towers or other instrumented locations for which data are readily available.

Figure 2.36 displays the real-time data acquisition and transmission design with local telemetry to the central recording building from where, via internet, data are transmitted to the Data Management Center (DMC) of IRIS (Incorporated Research Institutions for Seismology [www.iris.washington.edu]). In this case, streaming data stored at buffer of DMC can be obtained by anyone. Figure 2.37 shows a 267 s window of streamed data that was obtained from the DMC and re-plotted to show an event and a sizeable ambient response of the bridge. With the state-of-the-art sensor and recorders, the monitoring system at this bridge can be configured as a health monitoring system.

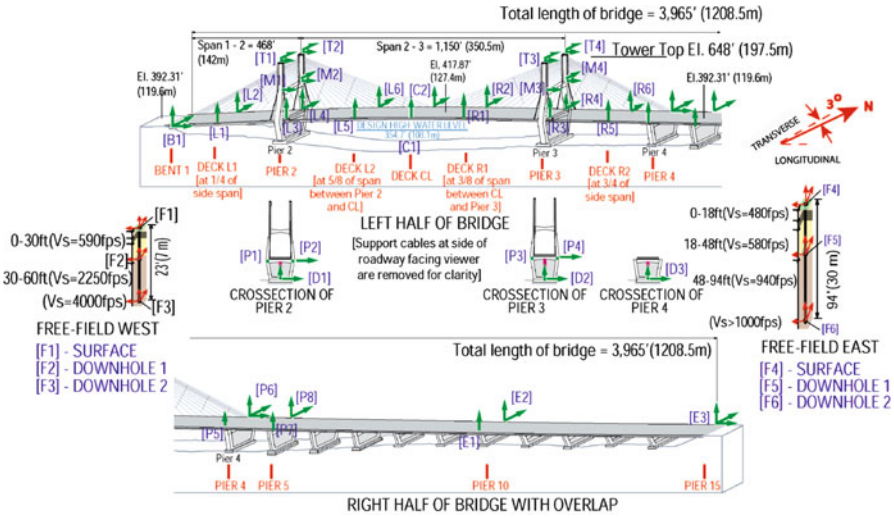

Fig. 2.35 Example of extensively instrumented cable-stayed Bill Emerson Memorial Bridge (also known as Cape Girardeau Bridge) (Missouri, USA) that has real-time streaming of responses

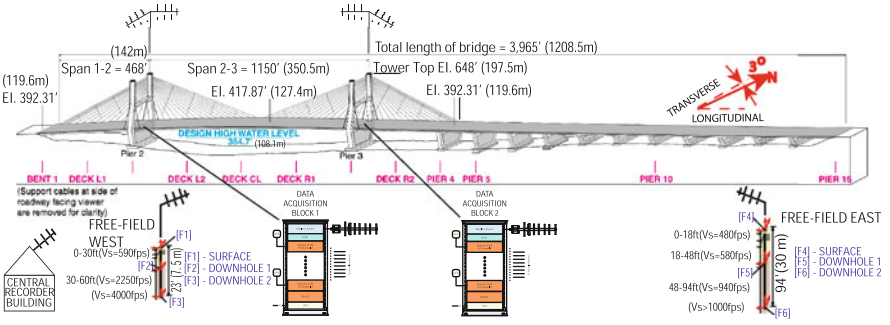

Fig. 2.36 Data acquisition units at different locations of the bridge and local telemetry set-up transmitting data to central recording building

2.7 Wireless Sensors

As previously mentioned, within the last decade, there has been intensive efforts to develop wireless sensors – the main motivation being to eliminate in seismic (and other) monitoring projects expensive costs to use cables required to connect the accelerometers (or other sensors) distributed at various floors and locations of a structure to a central location where the recorders are housed. At a central recorder location of most cable-connected monitoring projects, usually AC power is available to constantly charge packages of (normally 12-V) batteries as back-up power

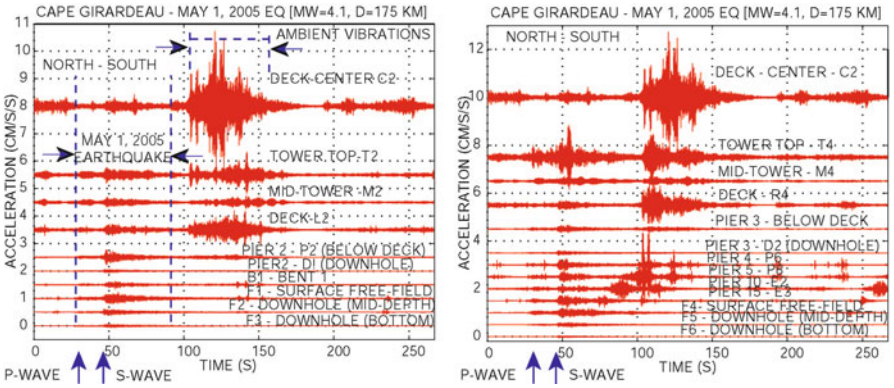

Fig. 2.37 Re-plotted from streamed data displaying response of the bridge to May 1, 2005 event (between 30 and 130 s of the 267 s record) that occurred at 175 km away. The plot also displays important ambient response that is caused by tower, cable and deck interaction

Fig. 2.38 Densely instrumented cable-stayed 2nd Jindo Bridge in South Korea uses wireless sensors (Photo courtesy of B. Spence, 2011)

supply to the sensors and recorders. Main obstacle to developing wireless sensors has been the power supply. Other issues related to A/D boards are solvable.

Using AC supply to constantly charge batteries at many locations of a structure and power individual sensors at those locations voids the definition of "wireless" as special safety designs must be incorporated when 110–220 V are directed to where the sensors are. Thus, most wireless sensors developed to date have been for short duration applications (*e.g.* laboratory tests). However, recently, 5-year battery life has been achieved. In combination with solar panels, such sensors promise to be useful in some applications (*e.g.* dams and bridges where solar panels can be easily utilized). Recently, wireless sensors have been deployed on the long span cable-stayed second Jindo Bridge in South Korea (Spencer and Yun 2010; Jang et al 2010

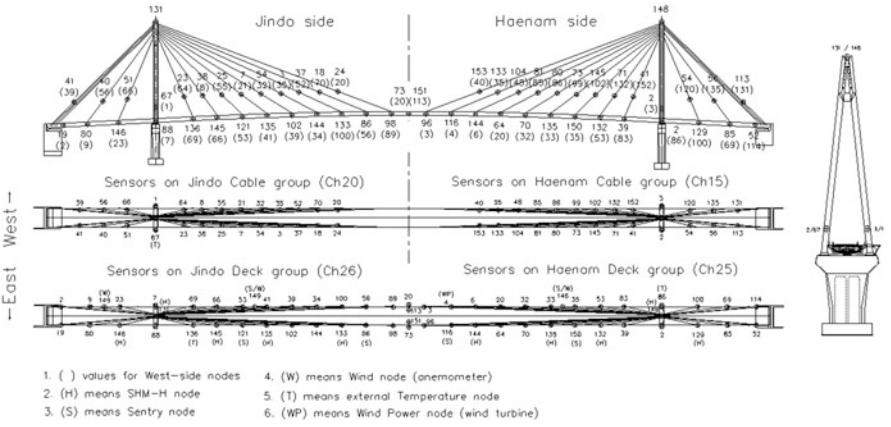

Fig. 2.39 Extensive sensor layout at 2nd Jindoa Bridge, South Korea. There are 113 nodes and each node has a tri-axial wireless sensor. Some nodes have other sensors as well (Figure courtesy of B. Spence, 2011)

and Cho et al. 2010). Figure 2.38 shows photo of the 2nd Jindo Bridge. Figure 2.39 shows extensive instrumentation on the bridge with wireless sensors.

2.8 Summary

In this paper, a summary of seismic monitoring as practiced in the past, as well as current applications and new developments to meet the needs of the engineering and user community is presented. Both historical and current trends and methods used for seismic monitoring of structures are discussed in terms of utilization of data acquired by seismic monitoring. The extent to which a structure should be instrumented to meet the code recommendations versus special needs are discussed without consideration of cost issues. Several examples of instrumented buildings are shown. Some of these examples of instrumented buildings are configured to obtain multiple types of response characteristics or phenomenon such as soil-structure interaction. A number of examples demonstrate the most recent applications that can be used for verification of design and construction practices as well as real-time applications for the functionality of built environment and assessment of damage conditions of structures.

Capitalizing on advances in computational and data transmission technology, it is now possible to configure and implement a seismic monitoring system for a specific building with the objective of rapidly obtaining and evaluating response data during a strong shaking event in order to help make informed decisions regarding the health and occupancy of that specific building.

Engineers increasingly demand approaches to measure displacements rapidly to be used for functionality assessments. On the other hand, dynamically measuring relative displacements between floors directly is very difficult and, except for tests

conducted in a laboratory (*e.g.*, using displacement transducers), has yet to be readily and feasibly achieved for a variety of real-life structures. However, recent technological developments have already made it possible to successfully develop and implement two approaches to dynamically obtain real-time displacements from which drift ratios or average drift ratios can be computed. New approaches in monitoring (using GPS technology and real-time double-integration) and related data acquisition systems to meet the special needs in obtaining displacements and, in turn, drift ratios, in real-time or near real-time are introduced. Thus, once drift ratios can be readily computed in near real-time, technical assessment of the damage condition of a building can be made since several threshold stages at which damage condition of a story as defined by drift ratios are pre-computed using relevant parameters of the type of connections and story structural characteristics including its geometry. Both approaches can be used for performance evaluation of structures and can be considered as building health-monitoring applications. Specific examples are provided for GPS and double integration applications.

Although there are other significant developments, there are still outstanding needs that require further development even though they have not been discussed herein. For example, two such needs are: (a) development of wireless instrumentation and (b) inexpensive sensors to deploy in large quantities in each selected building and in large number of selected buildings in an urban environment. The case for wireless instruments has been around for a while. New example of recent application of a long-span cable-stayed bridge equipped with wireless sensors powered by "5-year life" batteries combined with solar panels is reported. Such applications are practical for bridges and dams where solar panels can be deployed. However, the lack of much longer-life (in terms of decades) DC power supplies that can be used to power the instruments deployed in numerous locations of a building, inhibits its current usefulness in buildings and further development.

References

Abrahamson NA, Silva WJ (1997) Empirical response spectral attenuation relations for shallow crustal earthquakes. Seismol Res Lett 68:94–127

ANSS – An Assessment of Seismic Monitoring in the United States – Requirement for an Advanced National Seismic System (1999) U.S. Geological Survey, Circular 1188, 1999. http://earthquake.usgs.gov/monitoring/anss/, Accessed January 27 2011

Applied Technology Council (ATC) (1989) Procedures for post-earthquake safety evaluation of buildings. ATC-20, Redwood City

Applied Technology Council (ATC) (1997) NEHRP commentary on the guidelines for the seismic rehabilitation of buildings, prepared for the building seismic safety council, published by the Federal Emergency Management Agency, FEMA 274, Washington, DC

Astaneh A, Bonowitz D, Chen C (1991) Evaluating design provisions and actual performance of a modern high-rise steel structure. In: Seminar on seismological and engineering implications of recent strong-motion data. California Department of Conservation, Division of Mines and Geology, Sacramento, pp 5–1–5–10

Boore DM, Joyner WB, Fumal TE (1997) Equations for estimating horizontal response spectra and peak acceleration from western North American earthquakes: a summary of recent work. Seismol Res Lett 68:128–153

Borcherdt RD (1993) On the estimation of site-dependent response spectra. In: Proceedings of the international workshop on strong-motion data, Menlo Park, published By Port and Harbor Research Institute, Japan, (Preprint of manuscript submitted as "Simplified site classes and empirical amplification factors for site-dependent code provisions", for Proceedings of the NCEER, SEAOC, BSSC workshop on site response during earthquakes and seismic code provisions, University of Southern California, Los Angeles, 18–20 November 1992) vol 2, pp 399–427

Borcherdt RD (1994) Estimates of site-dependent response spectra for design (methodology and justification). Earthq Spectra 10:617–653

Borcherdt RD (2002a) Empirical evidence for acceleration-dependent amplification factors. Bull Seismol Soc Am 92:761–782

Borcherdt RD (2002b) Empirical evidence for site coefficients in building-code provisions. Earthq Spectra 18:189–218

Boroschek RL, Mahin S (1991) An investigation of the seismic response of a lightly-damped torsionally-coupled building, University of California, Berkeley, California, Earthquake Engineering Research Center Report 91/18, December, 291 p

Boroschek RL, Mahin SA, Zeris CA (1990) Seismic response and analytical modeling of three instrumented buildings. In: Proceedings of the 4th U.S. national conference on earthquake engineering, vol 2, Palm Springs, CA, 20-24 May. EERI, El Cerrito, pp 219-228

Building Occupancy Resumption Program (BORP) (2001) City and County of San Francisco, Department of Building Inspection, Emergency Operation Plan, (Rev. 2001). www.seaonc.org/member/committees/des_build.html

Campbell KW (1997) Empirical near-source attenuation relationships for horizontal and vertical components of peak ground acceleration, peak ground velocity, and pseudo-absolute acceleration response spectra. Seismol Res Lett 68:154–179

Çelebi M (1993) Seismic response of eccentrically braced tall building. ASCE J Struct Eng 119 (4):1188–1205

Çelebi M (1994) Response study of a flexible building using three earthquake records. In: Proceedings of the ASCE Structures Congress XII '94, Atlanta, GA, April 24–28, vol 2. American Society of Civil Engineers, New York, pp 1220–1225

Çelebi M (1995) Successful performance of base-isolated hospital building during the 17 January 1994 Northridge earthquake. J Struct Des Tall Build 5:95–109

Çelebi M (1996) Comparison of damping in buildings under low-amplitude and strong motions. J Wind Eng Ind Aerodyn [Elsevier Science] 59:309–323

Çelebi M (1997) Response of olive view hospital to Northridge and Whittier earthquakes. ASCE J Struct Eng 123(4):389–396

Çelebi M (1998) Performance of building structures – a summary. In: Çelebi M (ed) The Loma Prieta, California, earthquake of 17 October 1989 – Building structures, USGS prof. paper 1552-C, January 1998. US GPO, Washington, DC, pp c5–c76

Çelebi M (2000) Seismic instrumentation of buildings, U.S. geological survey open-file report 00–157

Çelebi M (2001a) Current practice and guidelines for USGS instrumentation of buildings including federal buildings. In: Cosmos Proceedings of the invited workshop on strong-motion instrumentation of buildings, Emeryville, November 2001, Cosmos publication No: CP-2001/04

Çelebi M (2001b) Current and new trends in utilization of data from instrumented structures. In: Çelebi MK [Editor with co-editors Erdik M, Mihailov V, Apaydin N], Strong-motion instrumentation for civil engineering structures, NATO science series-BOOK (E: Applied sciences-vol 373), Kluwer Academic Publishers, ISBN 0-7923-6916-5, pp 179–194

Çelebi M (2003) Identification of site frequencies from building records. Earthq Spectra 19(1):1–23

Çelebi M (2006a) Recorded earthquake responses from the integrated seismic monitoring network of Atwood building, Anchorage, (AK). Earthq Spectra 22(4):847–864, November 2006

Çelebi M (2006b) Real-time seismic monitoring of the new Cape Girardeau (MO) Bridge and preliminary analyses of recorded data: an overview. Earthq Spectra 22(3):609–630, August 2006

Çelebi M (2007) On the variation of fundamental frequency (period) of an undamaged building – a continuing discussion. In: Proceedings [CD] of the international conference on Experimental Vibration Analysis for Civil Engineering Structures (EVACES'07), Porto, Portugal, October 2007, pp 317–326, 24–27

Çelebi M (2008) Real-time monitoring of drift for occupancy resumption. In: Proceedings of the 14WCEE, Beijing, China, 13–17 October 2008

Çelebi M (2009) Seismic Monitoring to assess performance of structures in near-real time: Recent Progress, Chapter 1 in Seismic Risk assessment and Retrofitting, Geotechnical, Geological and Earthquake Engineering, Springer Publishing ISSN: 1573-6059, pp 1–24

Çelebi M, Liu H-P (1996) Before and after retrofit – response of a building during ambient and strong-motions. 8th US national conference on wind engineering, The John Hopkins University, Baltimore, 5–7 June

Çelebi M, Safak E (1991) Seismic response of Transamerica building–I, data and preliminary analysis. ASCE J Struct Eng 117(8):2389–2404

Çelebi M, Sanli A (2002) GPS in pioneering dynamic monitoring of long-period structures. Earthquake Spectra 18(1):47–61

Çelebi M, Safak E, Brady G, Maley R, Sotoudeh V (1987) Integrated instrumentation plan for assessing the seismic response of structures – a review of the current USGS program. USGS Circular 947

Çelebi M, Bongiovanni G, Safak E, Brady G (1989) Seismic response of a large-span roof diaphragm. Earthq Spectra 5(2):337–350

Çelebi M (compiler), Lysmer J, Luco E (1992) Recommendations for a soil-structure interaction experiment report based on a workshop held at San Francisco, California on February 7, 1992, U.S. Geological Survey open-file report, pp 92–295

Çelebi M, Phan LT, Marshall RD (1993) Dynamic characteristics of five tall buildings during strong and low-amplitude motions. J Struct Des Tall Build [Wiley] 2:1–15

Çelebi M, Presscott W, Stein R, Hudnut K, Wilson S (1997) Application of GPS in monitoring tall buildings in seismic areas, Abstract, AGU meeting, San Francisco, December 1997

Çelebi M, Presscott W, Stein R, Hudnut K, Behr J, Wilson S (1999) GPS monitoring of dynamic behavior of long-period structures. Earthq Spectra 15(1):55–66

Çelebi M, Sanli A, Sinclair M, Gallant S, Radulescu D (2004) Real-time seismic monitoring needs of a building owner and the solution – a cooperative effort. Journal of EERI, Earthquake Spectra, 20(2):333–346, May 2004

Çelebi M, Toksoz N, Buyukozturk O (2011) Revelations from ambient shaking data of a recently instrumented unique building at MIT Campus. Paper for IOMAC 2011 (International operational modal analysis conference), Istanbul, Turkey

Cho S, Jo H, Jang S, Park J, Jung H-J, Yun C-B, Spencer Jr, BF, Seo J-W (2010) Structural health monitoring of a cable-stayed bridge using wireless smart sensor technology: data analyses, University of Illinois, Urbana-Champaign, NSEL report series no. NSEL-024, June 2010, pp 461–480

Chopra A, Goel RK (1991) Evaluation of torsional provisions of seismic codes. ASCE J Struct Eng 117(12):3762–3782

COSMOS (2001) Proceedings of invited workshop on strong-motion instrumentation of buildings. Publication no. CP-2002/04

Crosby P, Kelly J, Singh JP (2004) Utilizing visco-elastic dampers in the seismic retrofit of a thirteen story steel framed building. ASCE Structures Congress XII, Atlanta, vol. 2, pp 1286–1291

Crouse CB, McGuire JW (1996) Site response studies for purpose of revising NEHRP seismic provisions. Earthq Spectra 12:407–439

Darragh R, Cao T, Graizer V, Shakal A, Huang M (1994) Los Angeles code-instrumented building records from the Northridge, California earthquake of January 17, 1994: processed release no. 1", report no. OSMS 94–17, California strong motion instrumentation program, California Department of Conservation, 10 December 1994

De La Llera J, Chopra A (1995) Understanding of inelastic seismic behavior of symmetric-plan buildings. Earthq Eng Struct Dyn 24:549–572

Ghanem R, Shinozuka M (1995) Structural system identification I. Theory. J Eng Mech 121 (2):255–264

Hall JF, Heaton TH, Halling MW, Wald DJ (1996) Near-source ground motion and its effects on flexible buildings. Earthq Spectra 11(4):569–605

Hamburger RO (1997) FEMA-173 seismic rehabilitation guidelines: the next step – verification. In: Proceedings of the SMIP97 seminar on utilization of strong-motion data, California strong motion instrumentation program, Division of Mines and Geology, California Department of Conservation, Sacramento, pp 51–69

Hart G, Rojahn C (1979) A decision-theory methodology for the selection of buildings for strong-motion instrumentation. Earthq Eng Struct Dyn 7:579–586

Heo G, Wang ML, Satpathi D (1977) Optimal transducer placement for health monitoring. Soil Dyn Earthq Eng 16:496–502

Huang MJ, Shakal AF (2001) CSMIP building instrumentation measurements and objectives. In: Proceedings of the invited workshop on strong-motion instrumentation of buildings, COSMOS, Emeryville. November 2001, Cosmos publication no: CP-2001/04, pp 15–19

International Building Code (2000) International conference of building officials, Whittier and also 2003, 2006, 2009 editions

Jang S, Jo H, Cho S, Mechitov K, Rice JA, Sim S-H, Jung H-J, Yun C-B, Spencer, Jr, BF, Agha G (2010) Structural health monitoring of a cable-stayed bridge using smart sensor technology: deployment and evaluation, University of Illinois, Urbana-Champaign, NSEL report series report no. NSEL-024, June 2010, pp 439–460

Kelly J (1993) Seismic isolation, passive energy dissipation and active control. In: Proceedings of the ATC 17–1 seminar on state of the art and state of the practice of base isolation, vol 1, pp 9–22

Kelly JM, Aiken ID, Clark PW (1991) Response of base-isolated structures in recent California earthquakes. In: Seminar on seismological and engineering implications of recent strong-motion data, preprints: California Division of Mines and Geology, Strong Motion Instrumentation Program, Sacramento, pp 12-1–12-10

Kijewski-Correa T, Kareem A (2004) The height of precision: new perspectives in structural monitoring. In: Proceedings of the earth & space: 9th aerospace division international conference on engineering, construction and operations challenging environments, 7–10 March, Houston

Ljung L (1987) System identification: theory for the user. Prentice-Hall, Englewood Cliffs, NY

Marshall RD, Phan LT, Çelebi M (1992) Measurement of structural response characteristics of full-scale buildings: comparison of results from strong-motion and ambient vibration records, NISTIR report 4884. National Institute of Standards and Technology, Gaithersburg

Panagitou M, Restrepo JI, Conte JP, Englekirk RE (2006) Seismic response of reinforced concrete wall buildings, 8NCEE (paper no. 1494), San Francisco, 18–22 April 2006

Porter LD (1996) The influence of earthquake azimuth on structural response due to strong ground shaking. In: Eleventh world conference on earthquake engineering, Acapulco, Mexico (June), (No. 1623), Elsevier – Pergamon, Oxford (CD-ROM)

Rojahn C, Matthiesen RB (1977) Earthquake response and instrumentation of buildings. J Tech Counc, Am Soc Civ Eng 103:TCI, Proceedings paper 13393, pp 1–12

Rojahn C, Mork PN (1981) An analysis of strong-motion data from a severely damaged structure, the imperial county services building, El Centro, California. U.S. Geological Survey open-file report, pp 81–194

SAC Joint Venture (2000) Recommended post-earthquake evaluation and repair criteria for welded steel moment-frame buildings, Report prepared for the Federal Emergency Management Agency, FEMA 352, Washington, DC

Sadigh K, Chang C-Y, Egan JA, Makdisi F, Youngs RR (1997) Attenuation relationships for shallow crustal earthquakes based on California strong motion data. Seismol Res Lett 68:180–189

Şafak E (1999) Wave-propagation formulation of seismic response of multistory buildings. ASCE J Struct Eng 125(4):426–437, April 1999

Şafak E, Çelebi M (1991) Seismic response of Transamerica building–II: system identification preliminary analysis. ASCE J Struct Eng 117(8):2405–2425, August 1991

Shakal AF, Huang MJ, Rojan C, Poland C (2001) Selection and criteria for the selection of buildings for instrumentation. In: Proceedings of the invited workshop on strong-motion instrumentation of buildings, COSMOS, Emeryville, November 2001, Cosmos publication no: CP-2001/04, pp 5–14

Shinozuka M, Ghanem R (1995) Structural system identification I. Theory. J Eng Mech 121(2): 265–273

Sohn H, Farrar CR, Hemez FM, Shunk DD, Stinemate DW, Nadler BR (2003) A review of structural health monitoring literature: 1996–2001, Los Alamos National Laboratory report, LA-13976-MS, 2003

Spencer BF Jr, Yun C-B (eds.) (2010) Wireless sensor advances and applications for civil infrastructure monitoring. Newmark Structural Engineering Laboratory Report Series, no. 24 (http://hdl.handle.net/2142/16434)

Straser E (1997) Toward wireless, modular monitoring systems for civil structures in John A 1079 Blume Earthquake Engineering Center Newsletter, No 2. Stanford University, Stanford, CA

Tarquis F, Roesset J (1988) Structural response and design response spectra for the 1985 Mexico City earthquake. University of Texas, Austin, Texas, report no. GD89-1, 208p

The MathWorks, Inc. (1988) User's guide: system identification toolbox for use with Matlab, South Natick, MA. (1988 and newer versions Uniform Building Code, International Conference of Building Officials, Whittier, CA. (1970 and, 1976, 1979, 1982, 1985, 1988, 1991, 1994, 1997 editions)

http://www.springer.com/978-94-007-5181-1

Earthquakes and Health Monitoring of Civil Structures

Garevski, M. (Ed.)

2013, XII, 331 p., Hardcover
ISBN: 978-94-007-5181-1